INS Report INS-R--348

AN ASSESSMENT OF THE INVENTORY OF CARBON-14 IN THE OCEANS

by

K.R. Lassey, M.R. Manning and B.J. O'Brien

Institute of Nuclear Sciences, D.S.I.R.,
Lower Hutt, New Zealand

This report was prepared for and was supported
by the International Atomic Energy Agency
under Technical Contract no. 4400/TC

AN ASSESSMENT OF THE INVENTORY OF CARBON-14 IN THE OCEANS

1. INTRODUCTION

1.1 Background

This report summarises the carbon-14 data in the world's oceans. The interest of the IAEA and UNSCEAR is ultimately to be able to predict more precisely what future radiation doses to man would be from the discharges into the earth's environment of man-made and naturally produced ^{14}C.

The report presents information published on oceanic ^{14}C concentrations and reviews several studies in which this data is used to estimate ^{14}C inventories in different regions of the ocean. Estimated inventories are given for ^{14}C of both natural and man-made origin, man made ^{14}C coming from atmospheric nuclear weapon tests and from nuclear power reactors. Data are also presented on the flux rates of ^{14}C between the atmosphere and the ocean.

1.2 Scope of Report

The only three significant sources of ^{14}C into the environment at this time are (a) that produced naturally by cosmic rays in the earth's atmosphere; (b) that produced since 1945 by explosion of nuclear weapons in the atmosphere; and (c) more recently an increasing input into the environment from the nuclear fuel cycle, associated with fission reactors used to produce electricity.

There have been numerous measurements of ^{14}C concentrations in the ocean, both in surface waters and at depth. However, these measurements have all been made since both the atmosphere and the ocean were contaminated with ^{14}C from nuclear weapons explosions. Recent measurements of ^{14}C in corals has produced information on oceanic levels of ^{14}C prior to nuclear testing and even before there was significant dilution of ^{14}C from the burning of fossil fuels.

The present report discusses the input rates of ^{14}C, notably the natural production rate from cosmic ray neutrons in the stratosphere; the input into the atmosphere from atmospheric nuclear tests from the early 1950s until the present time; and finally, an estimate of the current input from the nuclear power industry.

In order to determine input flux rates into the ocean, it is essential to consider ^{14}C concentrations in the atmosphere and this is done in section 3 of the report.

In section 4, we present a summary of data from several extensive surveys of the oceans, resulting in estimates of both natural and man made ^{14}C inventories. In section 5, a short discussion of oceanic chemistry, as it affects the carbon cycle, is discussed, and some brief descriptions of models used to simulate carbon exchange between the atmosphere and ocean.

2. THE CARBON CYCLE

The natural production rate of ^{14}C has not been precisely constant in the past, being effected by the earth's magnetic field and solar activity. Thus even the distribution of natural ^{14}C between and within the different carbon reservoirs on the earth is not in a steady state. It is also likely that this carbon cycle is effected by major oceanic circulation patterns which have changed in time.

In order to better understand the distribution of carbon and ^{14}C in the earth and within the ocean, and particularly to determine the dynamical features of the carbon distribution, several groups of researchers have developed mathematical models to simulate the movement of ^{14}C between the atmosphere, the biosphere, the ocean and within the ocean. Simple two box models and a variety of more complex models have been used over the past 30 years to determine exchange rates of carbon isotopes between the various earth reservoirs. The rate of injection of 'bomb' ^{14}C into the atmosphere from nuclear tests can only be inferred indirectly from concentration measurements made in the atmosphere and in the ocean, using mathematical models. Models have proved useful in representing the 'steady state' distribution of natural ^{14}C in the ocean, as well as the movement of 'bomb' ^{14}C through the ocean. Some of the inventory data and the flux rates referred to in this report have been arrived at through the use of models.

In modelling the carbon cycle on the earth, three main reservoirs of carbon are assumed, the ocean, the atmosphere and the biosphere.

The ocean contains some $37{,}000 \times 10^{15}$ gC, the atmosphere 615×10^{15} gC and the terrestial biosphere 800×10^{15} gC. Within humus, which is not assumed to be in exchange with the other reservoirs there is estimated to be 1500×10^{15} gC [Bolin et al., 1981]. The ocean is by far the largest carbon reservoir and most ^{14}C will eventually decay there. There are some 1000×10^{15} g of organic carbon within the ocean, the rest is in the form of dissolved inorganic carbon (DIOC). There is some 10 to 15 less DIOC in surface ocean waters than in deep water and this reduction in DIOC in surface waters plays an important role in setting the CO_2 concentrations in the atmosphere.

3. THE SOURCES OF RADIOCARBON

3.1 Natural ^{14}C Production

The ^{14}C isotope is produced continuously in the atmosphere by neutrons originating from cosmic rays. Low energy thermal neutrons and higher energy neutrons at resonance energies interact with atmospheric Nitrogen in the reaction

$$^{14}N + n \rightarrow {}^{14}C + p \qquad (3.1)$$

to yield ^{14}C atoms which are quickly oxidized to carbon monoxide and then to carbon dioxide. The ^{14}C isotope is radioactive and decays according to

$$^{14}C \rightarrow {}^{14}N + \beta \qquad (3.2)$$

with a half life of 5730 years (mean life 8267 years). As the lifetime of ^{14}C is long compared to the time scales of the physical and chemical processes that affect carbon, ^{14}C becomes widely distributed in the atmosphere, biosphere and oceans. However because of its low specific activity (about 13 Bq/gC), naturally produced ^{14}C in environmental carbon does not constitute a significant health risk due to the small radiation dose it produces.

The natural cosmogenic production of ^{14}C in the atmosphere increases with height. Approximately 65% of the production is in the stratosphere, with the remaining 35% being in the troposphere and predominantly the upper troposphere [O'Brien 1979]. Estimates of current cosmogenic production rates based on cosmic ray flux studies [O'Brien, 1979, Lingenfelter and Ramaty, 1970] or on measurements of the specific activity of ^{14}C [Damon et al., 1978; Grey 1972; Suess, 1965] give values consistent within uncertainties, ranging from 2.8×10^{26} atoms/annum to 3.5×10^{26} atoms/annum. Generally the lower end of this range is favoured by carbon cycle modelling studies.

In principle it is straightforward to calculate the total global inventory of ^{14}C from its production rate and mean life before decay. However to do this accurately one must take into account variations in production rate over the last 70,000 years or so. In fact the cosmic ray flux at the earth, and hence the cosmogenic ^{14}C production rate, over this time scale has been modulated by several factors. Principally these are a cycle in the earth's magnetic field strength with a period of 9000 years, and the solar sunspot cycle with a period of 11 years.

The geomagnetic field fluctuates by about 50% of its current value which is close to the average. As the strength of the geomagnetic field increases, the ^{14}C production rate decreases, and vice versa. The amount of ^{14}C in the atmosphere follows this cycle in production rate fairly closely and so is currently about average for geological time scales, while it was significantly higher 5000 years ago.

The global ^{14}C inventory fluctuations driven by the geomagnetic field cycle are considerably damped and lagged as the mean life of ^{14}C is comparable with the period of the forcing cycle. Variation of the global inventory I(t) can be modelled approximately by the equation

$$dI/dt = -\mu\ I + Q\ (1 + \tfrac{1}{2}\ \mathrm{Sin}(wt)) \qquad (3.3)$$

where μ is the ^{14}C decay rate ($1/8267\ yr^{-1}$), Q is the mean production rate, $w = (2\pi/9000)\cdot yr^{-1}$, and t is time in years. Ignoring transients the solution of this equation is

$$I(t) = (Q/\mu)\ (1 + (\mu/2\sqrt{\mu^2+w^2})\mathrm{Sin}(wt-\theta)\ ) \qquad (3.4)$$

where the phase lag θ is given by $\mathrm{Sin}(\theta) = w/\sqrt{\mu^2+w^2}$.

The above analysis implies that the global ^{14}C inventory will vary by about 8.5% about its mean value with a phase lag of about 80° from the geomagnetic field cycle. The global cosmogenic inventory at present is then close to its lowest value which, using the low end of the range of production rates given above, is 22000×10^{26} atoms ^{14}C.

3.2 Transport of ^{14}C in the carbon cycle

Carbon dioxide in the atmosphere exchanges with dissolved carbon in the oceans and is incorporated into the biosphere by photosynthesis. The ocean contains most of the carbon that can potentially exchange with that in the atmosphere. However the bulk of this is in the deep ocean which exchanges carbon slowly over several hundred years with a well mixed surface ocean layer. This surface mixed layer of the ocean in turn exchanges carbon with the atmosphere with time scales of the order of 7 years.

Exchange with the biosphere is complex, involving a wide range of different mechanisms and time scales. However effects on a decadal time scale are governed by the locking up of atmospheric carbon in plant growth with subsequent release by plant decay. Leaf litter, some root decay and agricultural cropping gives rise to release within a year or two of photosynthesis, while dying forest trees etc give rise to release several decades after photosynthesis.

We consider here exchange between the atmosphere and ocean mixed layer in just sufficient detail to show how the cosmogenic atmospheric ^{14}C inventory is determined.

The rate of change of the ^{14}C inventory in the atmosphere is given by combining the production rate, the loss due to flux into the oceans, the gain due to the reverse flux, and radioactive decay. This can be written

$$d(N_aA_a)/dt = Q + k_{ma}N_mA_m - k_{am}N_aA_a - \mu\ N_aA_a \qquad (3.5)$$

where Q is the production rate, k_{ma} and k_{am} are exchange rate coefficients for the flux from mixed layer to atmosphere and the reverse flux, N and A are the corresponding mass inventories and ^{14}C ratios, and μ is the radioactive decay rate. For a mass balanced exchange we must have

$$k_{ma}N_m = k_{am}N_a \tag{3.6}$$

and writing the ^{14}C inventory N_aA_a as I, it follows that

$$dI/dt = Q - [k_{am}(1 - A_m/A_a) + \mu] I. \tag{3.7}$$

This equation can be used to relate the equilibrium inventory to the production rate by setting the RHS to zero.

On average the carbon in the surface ocean is about 400 years old which means that the ^{14}C ratio $A_m = 0.95A_a$. Using the Oeschger et al., [1975] model estimate of $k_{am} = 1/7.3\ yr^{-1}$ the above equation leads to $I = Q \times 144yr$. With the lower range of the production rates given above this gives an atmospheric cosmogenic inventory of 400×10^{26} atoms ^{14}C.

If exchange between the atmosphere and biosphere is added to this simple picture, then the effective mean residence time of ^{14}C in the atmosphere will be decreased. However the effect is small as the ^{14}C returning from the biosphere is young and has almost the same ^{14}C ratio as atmospheric carbon.

A more direct approach to estimating the atmospheric cosmogenic inventory would be to use measurements of ^{14}C content in the atmosphere prior to the nuclear weapons era. As ^{14}C measurements have only been made from 1954 onward, proxy measurements have to be used, but these are readily available in tree rings that grew prior to 1945 [e.g. Stuiver and Quay, 1980].

The difficulty with this approach is that the ^{14}C activities available are all surface measurements, and vertical profiles in the atmosphere have to be assumed. If one assumes the atmosphere to be well mixed over the time scales of exchanges into other carbon reservoirs, then the ^{14}C content can be assumed to be constant. On this basis the ^{14}C inventory in 1940 would be estimated from the carbon inventory of 650×10^{15}gC with a ^{14}C content of 5.72×10^{10} atoms ^{14}C/gC giving $I = 372 \times 10^{26}$ atoms ^{14}C. Telegadas (1971) uses figures of $7? \times 10^{5}$ atoms ^{14}C/gAir for the 0.95 NBS Oxalic acid standard equivalent value, and an atmospheric mass of 5.2×10^{21}gAir. After allowing for a -3% Suess effect this gives 373×10^{26} atoms ^{14}C.

It is to be noted that these inventory estimates are about 10% lower than that derived above from the ^{14}C production rate and a box model. Some of this discrepancy might be due to ^{14}C ratios being higher in the upper troposphere and stratosphere than at the surface. Indeed Young [1967] and Telegadas [1971] have pointed out 2% variations between surface measurements and aircraft measurements in the lower troposphere.

Also Rafter and O'Brien [1970] note variations of 2% between Australian continental ^{14}C ratios and those at other South Pacific coastal sites.

3.3 Bomb ^{14}C

Testing nuclear weapons in the atmosphere since 1945 has produced additional ^{14}C in an amount slightly exceeding the natural cosmogenic atmospheric inventory.

The intense neutron fluxes produced by nuclear explosions give rise to ^{14}C via the same mechanism as cosmic ray neutrons. Early estimates of the amount of ^{14}C produced were based on estimates of the number of neutrons produced per Mt of explosion, and of what proportion of these would react with atmospheric nitrogen atoms. An often quoted figure has been given by Machta [1963] of 2×10^{26} atoms ^{14}C per Mt. This figure would depend upon the nuclear reactions within the bomb, for example : fusion reactions produce on average more neutrons per Mt than fission reactions [Glasstone and Dolan, 1977]. It is likely that much of the ^{14}C yield came from the final stage of fission-fusion-fission bombs.

Surface bursts are rated at half the nominal Mtonnage due to absorption of about half the neutron flux by the ground. However in all cases estimates of Mtonnage must be treated with caution. In fact early estimates of ^{14}C yield from nuclear explosions were obtained to assess health risks and were probably biased towards being overestimates, to ensure that risk assessments were conservative.

An alternative and more reliable approach to estimating the bomb produced ^{14}C yield is taken by B.J. O'Brien in a report by UNSCEAR [1977] exploiting correlations between atmospheric ^{14}C to strontium-90 fallout measurements. Strontium has a short residence time in the troposphere and is a fairly unambiguous measure of fission yield in nuclear explosions. This approach gave an estimate of 570×10^{26} atoms ^{14}C for total production by nuclear weapons.

Enting and Pearman [1983] have used a one dimensional carbon cycle model in which the nominal Mtonnage of nuclear tests are used as input to determine bomb ^{14}C. The Machta estimate of 2×10^{26} atoms ^{14}C per Mt was explicitly varied to produce results from the carbon cycle model that best fit ^{14}C measurements. This procedure gave a revised estimate of 1.2×10^{26} atoms ^{14}C per Mt. The corresponding figure for total ^{14}C yield from nuclear weapons tests was 550×10^{26} atoms ^{14}C, which is remarkably close to the figure of O'Brien quoted above, given the quite different approaches used.

The bulk of Mtonnage of atmospheric nuclear tests occurred in 1961 and 1962, these two years accounting for over 70% of the total. Prior to this there had been an increasing number of tests from 1951 through to 1958, followed by a brief moratorium. Apart from these features in the record there has been a much lower level of testing throughout the period from 1945 to 1976, with rare explosions since then.

Data in this paper give the ^{14}C ratio relative to the 0.95 NBS oxalic acid standard for ^{14}C which is an estimate of pre-industrial atmospheric ^{14}C ratios. Explicitly

$$\delta^{14}C = (R/R_{std} - 1) \times 1000 \qquad (3.8)$$

where R is the $^{14}C/^{12}C$ ratio measured and R_{std} is that for the 0.95 NBS standard which is [Stuiver, 1980b]

$$R_{std} = 1.176 \times 10^{-12}. \qquad (3.9)$$

Usually $\delta^{13}C$ is also measured on the samples, relative to the PDB limestone standard; $\delta^{13}C$ is defined as,

$$\delta^{13}C = (R/R_0 - 1) \times 1000 \qquad (3.10)$$

where R and R_0 are the $^{13}C/^{12}C$ ratios of the sample and PDB limestone standard respectively. The $\delta^{13}C$ data are used to standardise the $\delta^{14}C$ data to a constant $\delta^{13}C$ value of $-25^{o}/_{oo}$. This standardised $\delta^{14}C$ is always expressed as $\Delta^{14}C$ which, following Stuiver and Polach [1977] and Stuiver [1980b] is defined by

$$(1 + 10^{-3}\Delta^{14}C) = (1 + 10^{-3}\delta^{14}C)\left(\frac{.975}{1 + 10^{-3}\delta^{13}C}\right)^2 \qquad (3.11a)$$

or, to first order,

$$\Delta^{14}C = \delta^{14}C - 2(\delta^{13}C + 25)(1 + 10^{-3}\delta^{14}C). \qquad (3.11)$$

Atmospheric ^{14}C ratios in 1940 were about $-30^{o}/_{oo}$ due to the Suess effect. The total atmospheric inventory of ^{14}C, ignoring the increase in atmospheric carbon due to fossil fuel burning, could be estimated by

$$I = 0.385\ (\Delta^{14}C + 1000) \times 10^{26} \text{ atoms } ^{14}C. \qquad (3.12)$$

Figure 3.1 shows stratospheric and tropospheric $\Delta^{14}C$ values inferred from figures given by Telegadas [1971] and values from surface measurements by Levin [1985] and Manning et al. [1986]. In order to show the individual data sets more clearly, smoothed curves have been plotted rather than the original data. Table 3.1 gives annual average inventories inferred from the data shown. Note that the inventory estimates in table 3.1 based on surface measurements are expected to be too low at least until 1975 due to higher $\Delta^{14}C$ values in the stratosphere than in the troposphere.

The stratospheric data given by Telegadas [1971] show some inconsistencies. For example the earliest values for atmospheric inventories

would imply very high ^{14}C yield per Mt detonated prior to 1955. Similarly some of the early tropospheric values given show far more variation from one 3 month period to the next than appear reasonable from later studies. These probably reflect the difficulty of obtaining reliable inventory estimates from relatively sparse data.

The problem of sparse data coverage is particularly relevant for stratospheric bomb ^{14}C inventories. This is because the mixing times in the stratosphere are around 2 years, which is similar to the exchange time into the troposphere. As a result isolated measurements in the stratosphere soon after a nuclear explosion may miss the new input entirely, and measurements a short while later detect only part of it.

The situation regarding bomb ^{14}C can be summarized as follows. Nuclear weapons testing in the atmosphere produced about 550 x 10^{26} atoms ^{14}C predominantly in 1961 and 1962. For a brief period this increased the atmospheric inventory to nearly double the natural cosmogenic inventory. The bomb-produced excess of ^{14}C in the atmosphere has now reduced to about 95 x 10^{26} atoms ^{14}C or 25% of the natural cosmogenic inventory. This bomb-produced excess is currently decreasing at the rate of about 6% per year.

3.4 The ^{14}C Production in Nuclear Reactors

It has been estimated that the production of ^{14}C by nuclear power reactors is about 2.0 x 10^{23} atoms per year per MW(e)-yr [UNSCEAR, 1982]. *This figure is assumed to be an average for the different types* of reactors now in use. Currently, there are some 240 MW(e) of power reactors in operation and this is estimated to produce 0.5 x 10^{26} ^{14}C atoms per year, or about 17% of the natural production rate. Not all ^{14}C produced in nuclear reactors has yet been released into the environment, as some of it remains in unreprocessed fuel. However, up to 1985, the total emission of ^{14}C from nuclear reactors is only of the order of 1% of the total input from nuclear tests.

TABLE 3.1

INVENTORIES OF BOMB ^{14}C IN THE ATMOSPHERE
(in 10^{26} atoms of ^{14}C)

Year	Bomb yield (Mt)[1]	Stratosphere[2] NH	Stratosphere[2] SH	Troposphere[3] NH	Troposphere[3] SH	Total[4]	Surface NH[5]	Surface SH[6]
(Pre-1955	14.94)							
55	3.04	35	18	21			0	-1
56	14.94	35	18	10	13	76	0	5
57	16.46	45	21	11	5	82	0	9
58	48.72	45	30	21	18	114	0	19
59	0.00	64	40	62	47	213	45	30
60	0.05	51	31	47	45	174	41	38
61	111.01	48	31	57	50	186	42	40
62	220.50	189	50	88	65	392	69	43
63	0.00	267	53	146	86	552	137	65
64	0.01	157	52	144	111	464	161	103
65	0.02	99	57	140	123	419	145	124
66	0.90	80	55	130	126	391	133	120
67	3.08			120	119		120	115
68	9.30			113	111		108	107
69	3.10	45	41	105	103	294	105	103
70	5.40						102	99
71	1.67						96	96
72	0.11						90	91
73	2.50						81	84
74	0.50						75	78
75	0.00						71	74
76	4.10						67	69
77	0.02						64	65
78	0.04						63	61
79	0.00						57	58
80	0.60						51	55
81	0.00						49	51
82	0.00						46	48
83	0.00						43	45
84	0.00							42
85	0.00							41

1 Figures taken from Enting and Pearman's [1982] summary of nuclear weapons testing.
2 Stratospheric measurements as reported by Telegadas [1971]
3 Tropospheric measurements from aircraft as reported by Telegadas [1971]
4 An estimate of total atmospheric inventory based on the preceeding 4 columns
5 Estimates of Northern Hemisphere (troposphere + stratosphere) inventory based on surface measurements of $\Delta^{14}C$ at Vermunt, Austria by Levin et al. [1985]
6 Estimates of Southern Hemisphere (troposphere + stratosphere) inventory based on surface measurements of $\Delta^{14}C$ at Wellington, New Zealand by Manning et al. [1986]

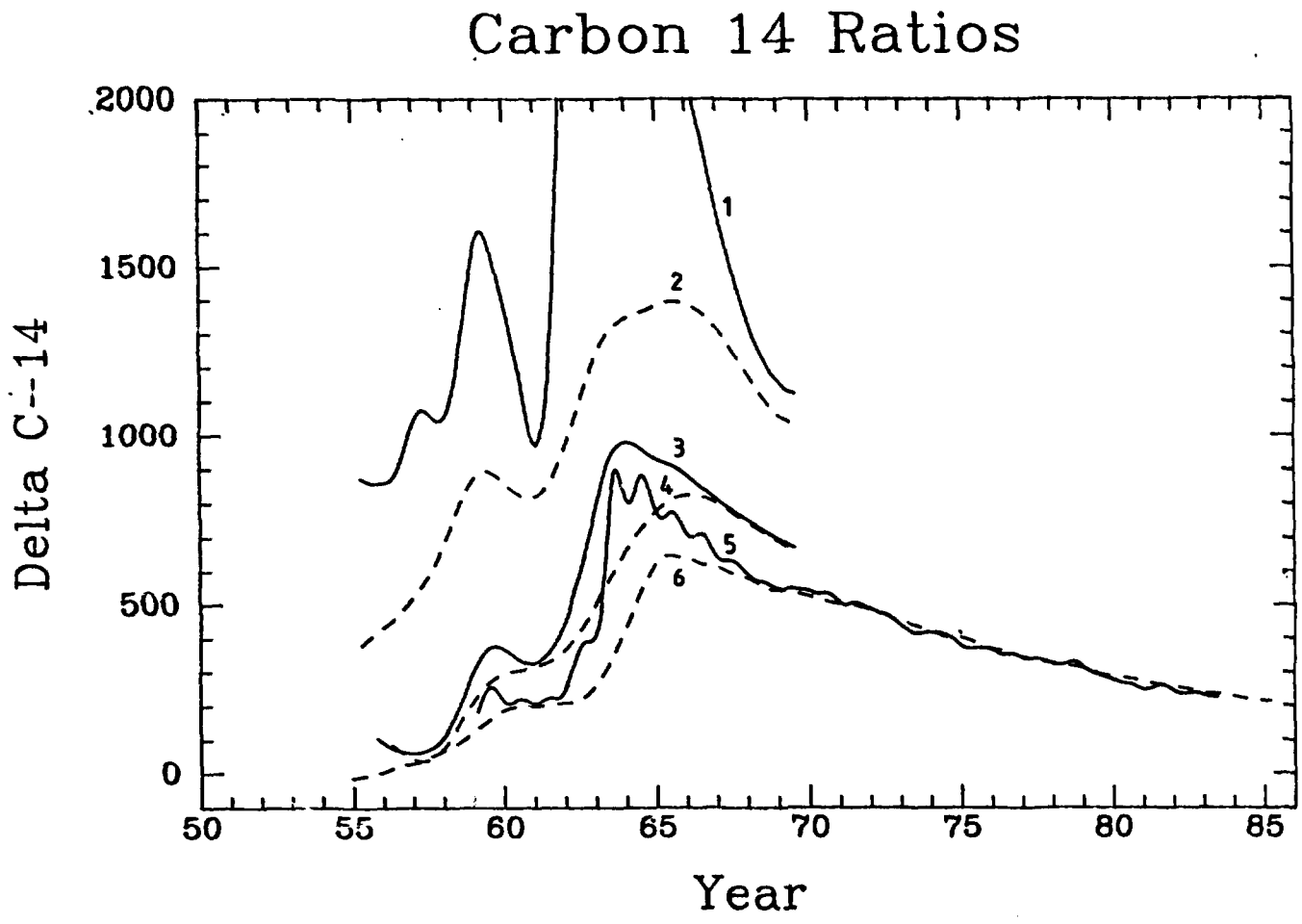

Fig. 3.1: $\Delta^{14}C$ excesses in the atmosphere as a result of nuclear bomb tests. Curves 1 and 2 are for the northern hemisphere (NH) and southern hemisphere (SH) stratospheres (respectively), after Telegades [1971]. Curves 3 and 4 are for aircraft measurements in the NH and SH tropospheres [Telegades, 1971]. Curves 5 and 6 are based on surface air measurements for the NH [Levin et al., 1985] and SH [Manning et al., 1986].

4. MEASUREMENTS OF RADIOCARBON IN THE OCEANS

In this chapter we examine the data base for radiocarbon in the world's oceans, and interpretations and analyses of that data. The oceans (a euphemism for all marine bodies) are subdivided geographically into three regions, termed the Atlantic, Pacific and Indian Oceans. These regions include those smaller marine bodies which are normally separately identified.

This chapter adopts the abbreviation DIOC for "dissolved inorganic carbon" (including the bicarbonate and carbonate ions) with $DIO^{13}C$ and $DIO^{14}C$ denoting the isotopically labelled species; their enclosure in square braces denotes a concentration. Pre-industrial values of $\Delta^{14}C$ are denoted $\Delta^{14}C^{\circ}$ and $\Delta^{14}C^{*}-\Delta^{14}C^{\circ}$ denotes a Suess-effected bomb component, also called a $\Delta^{14}C$ excess. All delta values are defined after Stuiver and Polach [1977].

4.1 Oceanic Surveys

Several systemstic surveys of oceanic radiocarbon have taken place in the last 15 years. The most extensive is the Geochemical Ocean Section Survey (GEOSECS) which extended throughout the 1970's and covered the major marine bodies. A section of the North Pacific Ocean was surveyed in detail as part of the NORPAX program in 1979. The Transient Tracers in the Ocean (TTO) program surveyed portions of the Atlantic Ocean in 1981-3.

All of the above surveys are discussed in more detail below, as is a project entitled "Radiocarbon in the Sea" conducted by A. W. Fairhall and collaborators between 1968 and 1975. Other reported surveys are of limited scope, exclude sampling at depth, or lack detailed analysis. Such other surveys, not further discussed, include:

- Linick [1978, 1980] who reports surveys by the La Jolla Radiocarbon Laboratory of the Pacific Ocean surface between 1957 and 1972, detailing the lateral transport of the bomb-carbon signal;
- Delibrias [1980] who reports several radiocarbon profiles taken in the southern Indian Ocean in 1973;
- Nydal et al. [1984] who report extensive surveys of carbon-14 in the ocean surface repeated over several years between 1966 and 1981. Extensive data are reported, emphasising the dispersal of the bomb-carbon signal.

4.1.1 The GEOSECS ocean surveys

The GEOSECS survey initiated in 1969 proceeded throughout the 70's to survey the chemical constituents of the world oceans. The objective was twofold: to provide a baseline study for future chemical changes; and to investigate large-scale oceanic transport and mixing processes. Measurements pertinent to radiocarbon determinations (including $\delta^{13}C$, $\delta^{14}C$ values and DIOC concentration) embrace only a few of the many geochemical species surveyed.

Following initial intercalibration [Craig and Weiss, 1970], surveys were conducted in the Atlantic and Pacific Oceans during 1972-3 and 1973-4 and in the Indian Ocean (with some Mediterranean and Red Sea stations) during 1977-8. The resulting radiocarbon results were reported by Stuiver and Ostlund [1980], by Ostlund and Stuiver [1980], and by Stuiver and Ostlund [1983], respectively.

A determination of DOI^{14}C distribution and an understanding of its sources, sinks and transport requires a good knowledge of physical oceanography. To the extent that radiocarbon measurements (especially the bomb component) are among the tracer information from which oceanographic data is obtained, the learning process is somewhat circular and iterative.

For example, the GEOSECS radiocarbon data has been used to deduce:

- upwelling rates and fluxes in the equatorial Atlantic necessary to account for depleted column inventories of DIO^{14}C (Broecker et al., 1978; Wunsch, 1984];
- mechanisms and magnitudes of vertical mixing in the Atlantic and Pacific thermoclines [Quay and Stuiver, 1980];
- Atlantic circulation patterns [Stuiver, 1980a];
- replacement times of Pacific, Atlantic and Indian abyssal waters of about 510, 275, 250 years, respectively [Stuiver et al., 1983];
- gross features of oceanic circulation and interactions with atmospheric CO_2 [Broecker et al., 1985].

A notable feature of all ^{14}C depth profiles (eg see Stuiver et al. [1981]) are the near-surface effects of "bomb carbon". Profiles of $\Delta^{14}C$ feature a pronounced peak at or near the surface of ~100°/$_{oo}$ or larger (see fig 4.1) which is attributed to an invasion of bomb-produced $^{14}CO_2$.

4.1.2 The NORPAX shuttle experiment (Leg 3)

This experiment surveyed the upper 1000m of a N-S section of the central equatorial Pacific Ocean (between Hawaii and Tahiti) in April 1979. Quay et al. [1985] report latitudinal variations in $\Delta^{14}C$ and in nutrient profiles from which are inferred equatorial upwelling rates and advective fluxes. The NORPAX results form a portion of the data interpreted by Broecker et al. [1985] (section 4.3.5).

4.1.3 The TTO program

This program was designed to trace the movement of man-made geochemical tracers (principally tritium and radiocarbon from weapons tests) into the Atlantic interior, and thereby provide a follow-up to the GEOSECS survey a decade earlier. Surveys of the North Atlantic and tropical Atlantic regions were conducted in 1981 and 1983, respectively. The data, so far incompletely analysed, are the subject of a sequence of 12 papers in the Journal of Geophysical Research volume 90, number C4,

commencing with an introductory summary by Brewer et al. [1985], and including an interpretive analysis by Broecker et al. [1985] which is the subject of section 4.3.5.

4.1.4 "Radiocarbon in the sea"

A. W. Fairhall of the University of Washington and his collaborators surveyed marine radiocarbon [Fairhall et al., 1972; Fairhall, 1971, 1974, 1975]; this followed a prior study of the fate of atmospheric bomb carbon which indicated a high rate of transfer to the oceans. The survey involved sampling marine waters (vertical profiles) at many locations from ships of opportunity between 1968 and 1975. A summary of the collected data is presented by Fairhall and Young [1985], along with miscellaneous earlier data as early as 1958. Analyses of this data noted the near constancy of the cosmogenic [DOI^{14}C] throughout the oceans; this point is taken up in section 4.3.4.

4.2 A Summary of Physical Oceanography

This section summarises the main physical features of oceanic circulation, providing background and jargon for succeeding sections.

The oceans occupy a surface area of about 3.6×10^{14} m^2 (71% of the earth's surface) with volume 1.35×10^{18} m^3, and mean depth therefore 3.7 km. Despite being relatively thin, the oceans are highly stratified. The well-mixed surface layer, homogenised vertically by wind and thermal stresses, varies between about 20 m and 200 m in depth, averaging about 75 m. It is deepest in the temperate regions (roughly delineated by 15-50°N and S) and somewhat shallower in both tropical and polar regions - in the latter of which it is barely discernible all year round [Bolin et al., 1981]. The mixed layer is underlain by the main thermocline with lower boundary typically 1km below the surface, and deepest also in the temperate regions.

The stratification follows isopycnal surfaces (constant density) which are deepest (i.e. the density gradients are lowest) in the temperate regions and noticeably shallower in the tropics (~15°S-15°N) [Broecker and Peng, 1981]. The isopycnal surfaces approach the polar surfaces where they may actually "outcrop" (i.e. intersect the ocean surface). Fig 4.2 illustrates these isopycnals for the Atlantic Ocean. Traditional oceanography describes sub-thermocline circulation as "thermohaline" - i.e. advection is driven along isopycnal surfaces by density gradients which in turn arise from temperature and salinity gradients.

The densest water is thus sourced near the poles from where it can flow equatorward and downward (along isopycnal surfaces) - particularly during winter when outcropping is more prominent. All the major oceans (Atlantic, Pacific, Indian) are thus fed with deep water from the easterly Antarctic circumpolar current (ACC), whereas only the North Atlantic has ready access to northern polar waters. Consequently, the Atlantic Ocean exports some deep water to the Indian and thence to the Pacific Oceans via the ACC, with compensatory counterflow of warmer thermocline water [Gordon, 1986]; fig 4.3 depicts these currents. The deep Atlantic is thus a nett exporter of water to the ACC, a picture supported by Δ^{14}C measurements [Stuiver et al., 1983].

The relative shallowness of tropical isopycnal surfaces indicates a nett upward advection (equatorial upwelling), with a downward advection (downwelling) in the neighbouring temperate regions [Broecker et al., 1978; Broecker and Peng, 1981]. Such advective fluxes are confirmed by $\Delta^{14}C$ values, which signify relative depletion and enhancement in these respective regions [Broecker et al., 1978, 1985; Stuiver, 1980a; Quay and Stuiver, 1980]. However, quantitative fluxes are not yet in concensus [Wunsch, 1984].

The temperate regions coincide with the gyre reservoirs, so named in recognition of the large-scale anticyclonic vortices which slowly stir the water in those regions.

4.3 Separation of Cosmogenic and Bomb Radiocarbon

It is well known that the natural isotopic composition of carbon in biospheric reservoirs has been appreciably perturbed by human activities. Declining $^{14}C/^{12}C$ ratios since ca. 1850 are due to the combustion of fossil fuels (free of ^{14}C). A concomitant decline in $^{13}C/^{12}C$ ratios is because fossil-fuel combustion and deforestation have both introduced isotopically lighter carbon into the CO_2 pool. However, it is the atmospheric testing of nuclear weapons since the mid 1950s that has most dramatically influenced $^{14}C/^{12}C$ ratios. This bomb-carbon influence extends to the terrestrial biosphere and surface ocean which both exchange CO_2 with the atmosphere on the decade time-scale. See Section 3.3 for more detail on bomb-carbon input.

The virtue of segregating the bomb contribution from the oceanic ^{14}C record is that the latter represents a useful tracer of oceanic DIOC (a tracer which is a non-ideal indicator of carbon exchange with the atmosphere: Broecker et al. [1980b]). Furthermore, validated models of the global carbon cycle should be able to account for both the near-steady cosmogenic ^{14}C distribution and the environmental response to the bomb-carbon signal. The terms "pre-industrial" and "cosmogenic" $DIO^{14}C$ are used as if synonymous, even though the recent history of the latter may be Suess-effected; see section 4.4 for more detail.

The segregation of the bomb and cosmogenic $DIO^{14}C$ is complicated by the sparsity of pre-nuclear $DIO^{14}C$ measurements. Some informed judgement then becomes necessary to infer or extrapolate to pre-nuclear levels, and to utilise retrospective measurements of ^{14}C levels captured in situ in banded corals. The following sections discuss the coral record, the extent of 1950s $DOI^{14}C$ measurements, some attempts to segregate the $DOI^{14}C$ record, and finally estimated inventories of the two $DIO^{14}C$ components.

4.3.1. The coral record

A convincing documentation of the Suess and nuclear effects in the surface ocean is recorded in banded corals, in much the same way as the atmospheric record is set in tree rings. These corals grow in many tropical and temperate areas and draw their carbonate skeleton from the DIOC of their host waters [Nozaki et al., 1978, Druffel and Linick, 1978; Druffel, 1980, 1981, 1982; Druffel and Suess, 1983]. That a reliable record of historic $\Delta^{14}C$ values for those host waters is thereby

laid down has been confirmed by cross-checking with historic oceanic records.

The coral record is a valuable aid to assessing the bomb-carbon history in local surface waters, by extrapolating the pre-nuclear era. The Suess effect does, however, complicate such extrapolation. Of necessity this technique is available only for certain coastal tropical and temperate environs where suitable corals grow. To date, ^{14}C histories have been reported in corals from Bermuda [Nozaki et al., 1978], from the Florida Straits [Druffel and Linick, 1978], from Belize [Druffel, 1980] and from the Galapagos Is. in the tropical Pacific Ocean [Druffel, 1981].

A summary of the coral $\Delta^{14}C$ record is displayed in fig 4.4.

4.3.2 Pre-nuclear oceanic carbon-14

Few oceanic ^{14}C measurements were taken before the nuclear era. Broecker et al. [1960] have summarised most of those available from the Atlantic Ocean and those early in the nuclear era (predating the significant bomb-carbon production of 1961-2). Data from the early 1960s in the Pacific and Indian Oceans are reported by Bien et al. [1965]. Other early Pacific data is reported by Linick [1978] and by Fairhall and Young [1985].

Killough and Emanuel [1981] have assembled a pre-industrial record sourced from Broecker et al. [1960] and from Bien et al. [1965], but in doing so discarded data for shallow waters likely to have been contaminated by bomb carbon. The assembly is matched to an assumed surface value of $\Delta^{14}C^{\circ} = -40^{\circ}/_{oo}$ citing Broecker et al. [1978] (who in turn cite Broecker and Li [1970]) for this value. See section 4.3.6 for more detail.

The $\Delta^{14}C^{\circ}$ value $-40^{\circ}/_{oo}$ is widely accepted as a reasonable average for the pre-industrial ocean surface. Broecker and Li [1970] proposed that value after surveying the pre-nuclear data; however, for reasons unstated, they excluded data taken poleward of 45° latitude. In an analysis of coral records, Druffel and Suess [1983] proposed $\Delta^{14}C^{\circ} = -40 \pm 2^{\circ}/_{oo}$ for the mid-gyre region of the North Atlantic and North Pacific Oceans, and an equatorial value of $-69^{\circ}/_{oo}$ (the latter based upon Galapagos Is corals). This reflects an expected latitudinal variation in $\Delta^{14}C^{\circ}$, with lower surface values in areas of upwelling, indeed values of less than $-100^{\circ}/_{oo}$ for southern ocean surfaces have been reported in references cited above. Broecker et al. [1979] have recently recommended $\Delta^{14}C^{\circ} = -45^{\circ}/_{oo}$ as an appropriate oceanic average.

In the pre-nuclear 1950s Suess-effected surface $\Delta^{14}C$ values in the range -50 to $-70^{\circ}/_{oo}$ are often cited for low and mid latitudes.

4.3.3 The Stuiver et al. analysis

Stuiver et al. [1981] summarised Atlantic and Pacific GEOSECS data into three latitude bands: equatorial (10°N-10°S), gyre (10°-50°N and S); the polar regions (latitude >50°) were not considered in detail. That summary is presented in fig 4.1.

The bomb carbon is segregated by assuming a pre-nuclear ocean surface with $\Delta^{14}C = -55‰$ for the gyre reservoirs and $-65‰$ for the equatorial zones, and by assuming that tritium penetration adequately portrays the penetration depth of radiocarbon. The resulting penetration depths are 1500m in the North Atlantic, 600m in the gyre reservoirs and 300m in the equatorial regions. The reconstructed pre-nuclear profiles are included on fig 4.1.

The ^{14}C concentration averaged in each latitude band in each of the two oceans is computed from the formula (with modified notation)

$$[DIOC]_S' = 1.176 * 10^{-12}(1 + 10^{-3}\Delta^{14}C)([DIOC]). \qquad (4.1)$$

Here, the molar concentrations $[DIO^{14}C]'_S$ and [DIOC] have the same units; the significance of the prime on the left-hand side is discussed in section 4.3.7.

The $DIO^{14}C$ concentrations are displayed in fig 4.5. Table 4.1 records the CO_2 invasion rates and column inventories of bomb carbon in each latitude band, as estimated by Stuiver et al. (the former from the atmospheric $\Delta^{14}C$ history in that latitude band). Also computed in table 4.1 are the bomb carbon inventories for the gyre and equatorial zones. The near equality of the average column inventories for the two oceans is noteworthy (though regions poleward of 50° are excluded). A rough estimate of the total oceanic inventory can be inferred by extrapolation of 82×10^{12} atoms(^{14}C)/m^2 to the world oceans, yielding 290×10^{26} atoms.

4.3.4 The Fairhall analysis

Fairhall and Young [1985] reported their results of oceanic DIOC surveys conducted in the early 1970s (see section 4.1.4). Those results included $\delta^{13}C$, $\delta^{14}C$, $\Delta^{14}C$ and the DIOC molarity as a depth profile at each of many oceanic stations. From each result was computed the "absolute ^{14}C concentration" (denoted herein as $[DIO^{14}C]_F'$) via the formula

$$[DIO^{14}C]_F' = 7.02 \times 10^8 \left(1 + \frac{\Delta^{14}C + 40}{1000}\right)([DIOC]) \text{ atoms } (^{14}C)/\ell, \qquad (4.2)$$

where [DIOC] is expressed in mmole/litre. In this formula it is said that "a value $-40‰$ is assumed for pre-industrial surface ocean water, and the specific activity of surface ocean water is taken to be the same as modern wood, i.e. equivalent to 5.85×10^{10} ^{14}C atoms/g(C)" [Fairhall, 1971]. The "Fairhall estimate" (4.2) exceeds by a factor 1.040 an estimate based on (4.1).

Fairhall noted that in deep oceans (e.g. below 1500m) where infiltration of bomb carbon should so far be minimal, $[DIO^{14}C]'_F$ was remarkably constant, and a value of $(1.42 \pm 0.02) \times 10^9$ atoms per litre was cited [Fairhall et al., 1972; Fairhall and Young, 1985]. Slightly

lower values were noted for the North Pacific's older water mass ($1.38x10^9$) and larger values for the North Atlantic ($1.47x10^9$), which may be contaminated at depth by bomb carbon. A summary of such profiles is presented as fig 4.6. Since, with measured surface DIOC concentrations of about 2.0 mmole/litre, the pre-industrial ocean surface is also compatible with $1.4x10^9$ atoms(^{14}C)/litre, Fairhall et al. conjectured that such near constancy must have featured throughout the pre-industrial ocean.

A conceptual difficulty with a universal ^{14}C concentration is the absence of an obvious mechanism for maintaining this balance. Fairhall [1974] explains this pre-industrial steady state as a balance between a downward rain of inorganic ($CaCO_3$) and organic detritus into the deep water where it dissolves, and an upward vertical diffusive flux driven by the DIOC concentration gradient. The two opposing fluxes are both of order 1 mole/yr/m^2 which, with the observed DIOC gradient in the thermocline, implies an acceptable diffusion coefficient of ~1 cm^2/sec. This nett detrital flux of ^{14}C is sufficient to balance decay and maintain its null gradient.

While Fairhall does not assess the oceanic cosmogenic inventory of $DIO^{14}C$, the straight-forward product of $1.42x10^9$ atoms/litre and oceanic volume ($1.35x10^{21}$ litre) suggests a cosmogenic inventory of $1.92x10^{30}$ atoms(^{14}C). However there remains a question-mark over the interpretation of equn (4.1): see section 4.3.7.

This purported separation of cosmogenic and bomb $DIO^{14}C$ led Fairhall [1971] to estimate a ca. 1970 oceanic bomb-carbon inventory of approximately $1.0x10^{14}$ atoms(^{14}C) per m^2 of ocean surface - viz, $3.6x10^{28}$ atoms(^{14}C) in total. This figure was compatible with Fairhall's apportioning of the bomb ^{14}C budget.

Craig [1969] had earlier observed a near constancy (to within 2%) of [$DIO^{14}C$] in abyssal North Pacific waters (below 1.5km), based on the data of Bien et al. [1965]. Craig reported an average "normalised concentration" of 4.2 cc/kg (using a formula of the form (4.1)) which translates to $1.36x10^9$ atoms(^{14}C)/litre. The equivalent Fairhall estimate would be $1.42x10^9$ atoms/litre. Craig interprets the near-null abyssal [$DIO^{14}C$] gradient as a coincidental balance between particulate delivery of cosmogenic ^{14}C and radioactive loss.

4.3.5 The Broecker at el. analysis

Broecker et al. [1985] sought to utilise the GEOSECS, NORPAX and TTO data to estimate an oceanic inventory of bomb carbon. A simplistic conceptualisation of oceanography and of CO_2 exchange (between atmosphere and surface ocean) permits a comparison between the invaded bomb $^{14}CO_2$ (from the atmosphere) and the in situ bomb-$DIO^{14}C$ (segregated from the total $DIO^{14}C$), so that an average invasion rate can be deduced. The systematic discrepancies which emerge between station-by-station inventories and invaded input then suggest how the oceanographic assumptions may be improved.

A bomb-carbon balance at the ocean-atmosphere interface requires a knowledge of the history of the $\Delta^{14}C$ excess (viz, $\Delta^{14}C^*$) in both the

atmosphere and ocean surface, along with the CO_2 invasion rate. Broecker et al. assume that the required atmospheric history is represented by the many reported surveys (fig 4.7a), and that the coral record provides sufficient information to estimate the ocean-surface history of $\Delta^{14}C^*$. By integrating each of these histories separately over each of the three major oceans, Broecker et al. estimate the corresponding ocean-average invasion rates. These rates (denoted I in the figures) are 22.3, 19.4 and 19.2 mole/m^2/yr for the Atlantic, Pacific and Indian Oceans, respectively.

The history of $\Delta^{14}C^*$ for the ocean surface is presumed to follow a universal shape (fig 4.7b) which is deduced from the coral record of the Florida Straits [Druffel and Linick, 1978]. In characterising the coral record of a single locality as typifying the bomb carbon throughout the ocean surface (to within a scale factor), Broecker et al. ignore as minor the cumulative effects of surface advection patterns over the nuclear era. A knowledge (or guesstimate) of $\Delta^{14}C^\circ$ together with a recent (e.g. GEOSECS) measurement then suffice to reconstruct the supposed bomb-carbon invasion history at each station.

A map of the segregated $\Delta^{14}C^*$ based on the GEOSECS surveys is presented as fig 4.8.

The bomb-carbon column inventories (i.e. inventories of unit oceanic columns) are shown in fig 4.9a. They are deduced from measured $\Delta^{14}C$ profiles at each station using the formula (with modified notation)

$$\Delta^{14}C = (\overline{[DIOC]})\times 10^{-3} \int_0^z \{ \Delta^{14}C(z') - \Delta^{14}C^\circ(z') \}\, dz'. \qquad (4.3)$$

Here, $\Delta^{14}C(z')$ and $\Delta^{14}C^\circ(z')$ are the ^{14}C content (per mil - hence the factor 10^{-3}) as measured, and as deduced for the pre-industrial era, at depth z'; the latter merges with the former at depth z (maximum contemporary bomb-carbon penetration depth) and is extrapolated to the surface value, itself reconstructed from the coral record - i.e. from fig 4.7b. The integral in (4.3) is the area between these two deptn profiles, one measured, the other reconstructed. The term $\overline{[DIOC]}$ is the average DIOC concentration down to depth z.

Broecker et al. subdivide each ocean into 5° latitude bands, and within each band estimate and tabulate both the bomb-carbon inventory and the bomb-carbon input. The latter is estimated from the local atmospheric $\Delta^{14}C$ record (fig 4.7a) and the ocean-average invasion rate, I. The inventory/input quotient then averages to unity in each ocean, and should permit comparison of the inventories in different oceans which are surveyed at different times. Fig 4.9b displays the world-wide GEOSECS inventories normalised in this way. The inventory/input quotients evidently exceed unity only in the temperate zones, which is attributed to the convergence and downwelling of surface water in these zones in conjunction with latitudinally variable invasion rates.

Inventories are tabulated in two different ways. The first (table 4.2a) facilitates comparison with table 4.1; such a comparison awaits

section 4.3.7. The second (table 4.2b) presents inventories and inputs in broad latitude bands which, according to fig 4.9b, mainly separate regions of excess inventory (over input) from those of deficit. The total inventory of 289×10^{26} atoms(^{14}C) updates an earlier estimate by Broecker, Peng and Enge [1980] of $(314 \pm 35) \times 10^{26}$ atoms based on a smaller data base.

The excesses and deficits of inventories over input evident from fig 4.9b and table 4.2b are in qualitative accord with prevailing oceanographic wisdom on invasion-rate variations and oceanic advection patterns. However, even with these patterns included, the model cannot account for the observed decline in atmosphere-borne fossil-fuel CO_2 [Peng, 1986].

4.3.6 The Killough and Emanuel data assemblage

Killough and Emanuel [1981] set out to compare the capabilities of several oceanographic models to account for the history of fossil-fuel transfer (as CO_2) to the oceans. In order to do this they calibrated each model by insisting that its steady state reproduces the pre-industrial distribution of $DIO^{14}C$. The data base assembled for this calibration can also serve to supply an estimated inventory of that pre-industrial $DIO^{14}C$.

From the data reported by Broecker et al. [1960] and by Bien et al. [1965] Killough and Emanuel assembled data for depths below 200m data from 191 locations: 81 from the Atlantic, 62 from the Pacific, and 48 from the Indian Ocean. The depth cut-off at 200m followed a recommendation by Bien and Suess [1967] that water below this depth was at that time uncontaminated by bomb carbon. Killough and Emanuel interpolate this data to a supposed $\Delta^{14}C^\circ = -40^\circ/_{oo}$ at the ocean surface.

Killough and Emanuel stratified the oceans into 19 horizontal layers (16 below 200m), and each $\Delta^{14}C$ datum was considered representative of the layer from which it was drawn. A depth profile of supposed pre-industrial radiocarbon was thereby assembled, embodying the assumption that $\Delta^{14}C^\circ$ decreased with depth. In their table 1 Killough and Emanuel cite the total carbon mass in each layer and the value of $(1 + \Delta^{14}C^\circ/1000)$. By summing over all layers one can infer the pre-industrial inventory implied by Killough's and Emanuel's calibration:

$$\sum'_{KE} {}^{14}C = R_{std} \, (N_o/12) \sum_i y^o_i \, (1 + 10^{-3} \, \Delta^{14}C^\circ_i). \qquad (4.4)$$

Here y^o_i is the total carbon mass (in gram) and the index i identifies the layer; $N_o = 6.023 \times 10^{23}$ is Avagadro's number, and the divisor 12 converts gram(C) to mole(C); $R_{std} = 1.176 \times 10^{-12}$ is the $^{14}C/C$ standard ratio. The pre-nuclear inventory estimated in this way is

$$\sum'_{KE} {}^{14}C = 1.90 \times 10^{30} \text{ atoms } (^{14}C).$$

4.3.7 Oceanic inventories of cosmogenic and bomb-produced radiocarbon

The $\delta^{14}C$ value is defined by equn(3.8). The $^{14}C/C$ ratio, R, of a sample is thus

$$R = R_{std} (1 + 10^{-3}\delta^{14}C). \quad (4.5)$$

The only assumption made is that there is no isotopic fractionation during the collection of a representative water sample and during its processing for isotopic determination. Thus, setting $R_{std} = 1.176 \times 10^{12}$,

$$[DIO^{14}C] = 1.176 \times 10^{-12} (1+10^{-3}\delta^{14}C)([DIOC]), \quad (4.6)$$

where the concentrations $[DIO^{14}C]$ and [DIOC] are in the same units (e.g. m.mole/litre). Integrating over the oceanic volume yields the the total $DIO^{14}C$ inventory.

Formula (4.6) contrasts with the formula usually adopted to compute the $DIO^{14}C$ content of an oceanic reservoir which has $\Delta^{14}C$ in place of $\delta^{14}C$; e.g. see Stuiver [1980b] and eqns (4.1), (4.4). Denote that analogue of (4.6) by $[DIO^{14}C]'$, viz:

$$[DIO^{14}C]' = 1.176 \times 10^{-12} (1+10^{-3}\Delta^{14}C)([DIOC]). \quad (4.7)$$

Whichever formula is the more appropriate depends upon the interpretation placed upon the result. Formula (4.6) correctly produces a reservoir inventory, subject only to no fractionation between collection and assay (inclusively). Formula (4.7) is appropriate for considering carbon transfer processes for which ^{14}C is merely a tracer and for which isotope fractionation occurs (and is quantifiable from the $\delta^{13}C$ values). The latter formula would then measure an apparant or fractionation-corrected radiocarbon content.

Although $\delta^{14}C$ is a more fundamental experimental result than $\Delta^{14}C$ of equn (3.11), it is the latter which is the more extensively reported. It is thus useful to relate (4.6) and (4.7):

$$[DIO^{14}C] = [DIO^{14}C]' \left(1 + \frac{10^{-3}\delta^{13}C}{1000}\right)^2, \quad (4.8)$$

which effectively reconstructs $\delta^{14}C$ from $\Delta^{14}C$.

Fortunately, oceanic values for $\delta^{13}C$ do not vary by more than a few parts per mil - much less than variations in $\Delta^{14}C$. Kroopnick [1974a, 1980] presents extensive $\delta^{13}C$ measurements (including GEOSECS) which are largely confined to the range -1 to $2^{o}/_{oo}$, with most in the range 0 to

1°/₀₀. Nozaki et al. [1978] report pre-industrial $\delta^{13}C$ values (back to ca. 1770), as laid down in Bermuda corals, of between about -0.5 and 0°/₀₀, falling towards -0.8°/₀₀ in modern times. Druffel [1982] reports $\delta^{13}C$ values in the range -1.0 to 0.6°/₀₀ in coral bands of the Florida Straits laid down since 1642. It is thus quite adequate to treat $\delta^{13}C$ as constant (and we take $\delta^{13}C = 0$) when volume-integrating $[DIO^{14}C]$ of equn (4.8) to form an oceanic inventory:

$$\sum^{14}C = (\sum'^{14}C)\left(1 + \frac{10^{-3}\delta^{13}C}{1000}\right)^2, \qquad (4.9)$$

Here, $\Sigma^{14}C$ is $[DIO^{14}C]$ integrated over the oceanic volume, and $\sum'^{14}C$ is the analogous integration of $[DIO^{14}C]'$.

Inventories already available but computed from $\Delta^{14}C$ values can thus be corrected by means of equn (4.9). An inventory deduced from the Fairhall estimate (4.2) requires an extra factor:

$$[DIO^{14}C]_F = 0.96[DIO^{14}C]'_F \left(1 + \frac{10^{-3}\delta^{13}C}{1000}\right)^2 \qquad (4.10)$$

The overall multiplier of $[DIO^{14}C]'$ is close to unity.

The above considerations apply to inventories calculated directly from $\Delta^{14}C$ or $\Delta^{14}C°$ which in turn are deduced, in practice or in principle, from $\delta^{14}C$ or $\delta^{14}C°$. The same formulae apply to bomb-carbon inventories provided only that differences between pre-industrial and modern values of $\delta^{13}C$ can be ignored. As noted above, such differences appear quite negligible.

Table 4.3 summarises estimates of radiocarbon inventories, as detailed in preceding sections. Each is adjusted to "uncorrect" for fractionation, with the assumption that $\delta^{13}C = 0$ represents a reasonable oceanic average.

Although a consensus of both cosmogenic and bomb-carbon inventories seem evident from table 4.3, it should be noted that:

- both bomb-carbon inventories rely heavily on the GEOSECS data. However, the detailed bomb-carbon distributions do vary (see tables 4.1, 4.2a), particularly for the Atlantic Ocean. Mid-latitude Pacific inventories are in reasonable accord at 82×10^{12} atoms per m^2 of surface, which equates well to the overall average. However, the two analyses (sections 4.3.3, 4.3.5) employ different rationales for segregating the the bomb ^{14}C from the $\Delta^{14}C$ record: Stuiver et al. presume a pre-nuclear base-line, the excess being the bomb component; Broecker et al. skim from the $\Delta^{14}C$ value an amount decreed by their universal coral curve (fig 4.7b) to represent the

bomb contribution. The near equality of the two bomb-carbon totals in table 4.3 is a cancellation of two effects: Stuiver et al. estimate a lower mid-Atlantic inventory (by about 10%); an extrapolation to the world ocean of the Stuiver et al. result overestimates the bomb carbon residing in the Antarctic and south Indo-Pacific Oceans.

- the two cosmogenic inventories are obtained in different ways from independently compiled data. Their corroboration is thus reassuring.

In parenthesis, it is appropriate to comment on the correction for fractionation embodied in $\Delta^{14}C$. The inherent assumptions are that disparate $^{13}C/C$ ratios between intimate carbon reservoirs accurately portray fractionation in the nett inter-reservoir transfer of carbon. In fact there may be different causes of $\delta^{13}C$ disparities. For example, Kroopnick [1974a, 1974b] has interpreted correlations between oceanic $\delta^{13}C$, dissolved oxygen and DIOC as indicating that a significant component of DIOC arises from oxidation of isotopically-lighter organic carbon ($\delta^{13}C = -23^{o}/_{oo}$). A significant organic source of DIOC would thereby depress $\delta^{13}C$ values and render them unreliable for indicating fractionation during ocean-atmosphere exchange. This consideration affects $\Delta^{14}C$ values, but not ^{14}C inventories computed from actual or reconstructed $\delta^{14}C$ values.

4.4 Temporal Variations in Oceanic Radiocarbon

"Pre-industrial" and "cosmogenic" ^{14}C distributions have been used as interchangeable terms, reflecting the reality that, to a good approximation, the latter is perpuated largely unchanged in time; the former is therefore just a 19th century sampling of the latter. Such variations as do occur in cosmogenic ^{14}C are related to extra-terrestrial modification of the cosmic-ray flux, or to terrestrial (e.g. magnetic) perturbations on that flux. In addition, cosmogenic ^{14}C has been slightly redistributed during the industrial era due to isotopic dilution by fossil-fuel carbon. See Chapter 3 for more detail.

The environmental response to the bomb-carbon signal will persist for centuries before environmental equilibration occurs (e.g. the turnover times of abyssal waters are of order 500 yr [Stuiver et al., 1983]). For most oceanic regions a comprehensive ^{14}C data set is available for only one isolated time (GEOSECS), precluding a time-series inventory. For certain regions a ^{14}C history is available, notably:

- in regions of banded coral growth (e.g. fig. 4.4).

- in extensive surface surveys over the period 1966-1981 by the Trondheim group [Nydal et al., 1984]. These show only a gradual decline, or no discernible decline at all, since the early 1970s, but do indicate strong seasonal effects - also noted by Broecker and Peng [1980].

- in regions where NORPAX and TTO surveys have provided a follow-up to the GEOSECS surveys. Broecker et al. [1985] in their fig 7 show the latitudinal variations in column inventories; their results are

compatible with no significant lateral movement of bomb carbon over the period between the surveys.

Post-GEOSECS history of bomb carbon can be expected to follow the circulation pattern outlined in section 4.2. Indeed, ^{14}C measurements have contributed to the knowledge of ocean circulation (leading to a somewhat iterative logic). Thus bomb carbon will slowly penetrate to the abyssal oceans via tha North Atlantic and Antarctic waters, in a time scale of about 500 years [Stuiver et al., 1983].

The evolving total inventory of oceanic radiocarbon is dictated by a balance between radioactive decay (0.012% p.a.) and continued invasion from the atmospheric reservoir. The latter is the subject of Chapter 5, but a quick estimate of the post-1972 invasion can be supplied here. Assume a globally-averaged CO_2 flux of 20 mole/yr/m^2 between air and sea-surface for which the $\Delta^{14}C$ difference exceeds the steady state value by ~150-200°/$_{oo}$ since 1972. This provides for an invasion of $(1.176 \times 10^{-12}) \times (150\text{-}200/1000) \times 20$ mole/yr/m^2 or 10×10^{26} atoms (^{14}C)/yr, about 3% of the present bomb-carbon inventory. Thus in the interim 1972-1985 the bomb-carbon inventory in the oceans has increased by about 40%. For a more detailed calculation, see section 5.5.

4.5 Spatial Variations in Oceanic Radiocarbon

The spatial distribution of cosmogenic ^{14}C seems surprisingly uniform throughout the oceans at around 1.4×10^9 atoms per litre, probably as a result of delivery rates closely matching the radioactive decay rate (section 4.3.4). Although this reported uniformity seems not to have been widely commented upon, some confirmation comes from noting that the resulting estimated inventory is in concordance with that deduced from Killough's and Emanuel's data (table 4.3).

Figs 4.8, 4.9 represent the best available portrayal of the gross bomb-carbon distribution, as of 1972. The spatial redistribution since that time is determined by ocean circulation, as discussed in section 4.4. A significant depletion in the average ocean-surface $DIO^{14}C$ is not likely to be detected until the difference between air and surface $\Delta^{14}C$ approaches its pre-industrial value of around 40°/$_{oo}$ - about a fifth of its current value.

Table 4.1

Atlantic and Pacific GEOSECS bomb-carbon inventories and CO_2 invasion rates summarised over mid latitude bands*

Zone	CO_2 invasion rate (mole/yr/m^2)	Water area (10^{12} m^2)	Col. inventory (10^2 atoms/m^2)	Inventory (10^{26} atoms)
Atlantic Ocean				
50°N-10°N	27.2	29.8	110	32.7
10°N-10°S	11.1	12.7	42	5.4
10°S-50°S	20.2	27.9	72	20.2
50°N-50°S	21.4	70.4	83	58.2
Pacific Ocean				
50°N-10°N	21.0	53.4	89	47.3
10°N-10°S	12.1	40.2	48	19.4
10°S-50°S	26.5	57.9	100	57.9
50°N-50°S	20.8	151.5	82	124.5

* The invasion rates and column inventories (in units μ mole/m^2) are reported by Stuiver et al. [1981], and the water areas by Broecker et al. [1985]; the inventories are computed here.

Table 4.2a

Bomb-carbon inventories calculated by Broecker et al. for mid-latitude Atlantic and Pacific Oceans*

Latitude	Atlantic Ocean		Pacific Ocean	
	Col. inventory (10^{12} atoms/m^2)	Inventory (10^{26} atoms)	Col. inventory (10^{12} atoms/m^2)	Inventory (10^{26} atoms)
50°N-10°N	122	36.5	93	49.4
10°N-10°S	30	3.8	50	20.1
10°S-50°S	86	24.0	94	54.7
50°N-50°S	91	64.3	82	124.2

* The latitude bands duplicate those of Table 4.1; the data is adapted from Broecker et al. [1985, Table 6]. All inventories estimated as of 1972.

Table 4.2b

Bomb-carbon Summary for Individual Ocean Regions Showing Either Excess or Deficient Inventories Relative to the Amount Expected if the CO_2 Invasion Rate Were Uniform Over the Ocean*

Latitude Band	Water Area (10^{12} m^2)	Inventory (10^{26} atoms)	Input (10^{26} atoms)	Inventory-Input# (10^{26} atoms)
		Atlantic Ocean (I = 22.3 mol/m^2/yr		
80°N to 40°S	18.6	26.6	19.7	+ 6.9
40°N to 20°N	15.8	23.0	14.5	+ 8.5
20°N to 20°S	26.7	10.8	23.1	-12.3
20°S to 45°S	18.4	18.5	14.2	+ 4.3
45°S to 80°S	15.1	5.2	12.6	- 7.4
80°N to 80°S	94.6	84.1	84.1	0.0
		Indian Ocean (I = 19.4 mol/m^2/yr)		
25°N to 15°S	27.0	13.2	24.1	-10.9
15°S to 45°S	29.8	40.5	20.3	+20.2
45°S to 70°S	20.7	15.9	25.2	- 9.3
25°N to 70°S	77.5	69.6	69.6	0.0
		Pacific Ocean (I = 19.2 mol/m^2/yr)		
65°N to 40°N	15.1	7.3	13.4	- 6.1
40°N to 15°N	35.0	35.9	27.8	+ 8.1
15°N to 10°S	50.0	23.7	39.1	-15.4
10°S to 55°S	63.0	61.3	43.6	+17.7
55°S to 80°S	13.8	6.6	10.9	- 4.3
65°N to 80°S	176.9	134.8	134.8	0.0
		World Ocean		
	349.0	288.5		-

* Table from Broecker et al. [1985] with corrections after Peng [1986]. All inventories estimated as of 1972.

\# The mean CO_2 invasion rate, I is adjusted for each ocean so that input matches inventory.

Table 4.3

Oceanic Radiocarbon Inventories

Source	Reference section	Inventory (10^{26} atoms)
Cosmogenic radiocarbon		
Fairhall et al.	4.3.3	1.93×10^{4}
Killough and Emanuel	4.3.5	1.99×10^{4}
Bomb carbon (as of ~1972)		
Stuiver et al. (extrapolated)	4.3.2	310
Broecker et al.	4.3.4	303

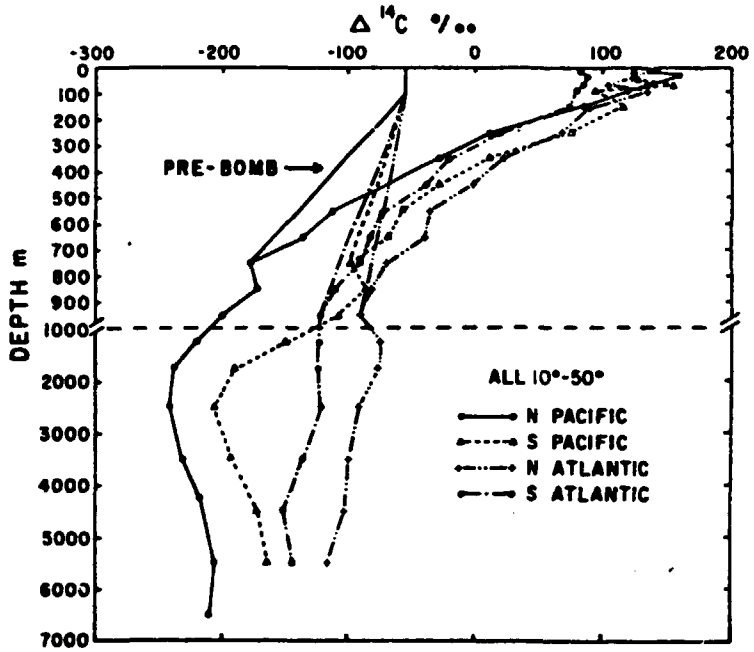

Fig. 4.1(a): $\Delta^{14}C$-depth profiles for the Atlantic and Pacific Ocean gyre reservoirs (10°-50° latitude). The assumed pre-bomb $\Delta^{14}C$-depth profiles all extend to $\Delta^{14}C = -55‰$ at the surface. (Taken from Stuiver et al. [1981]).

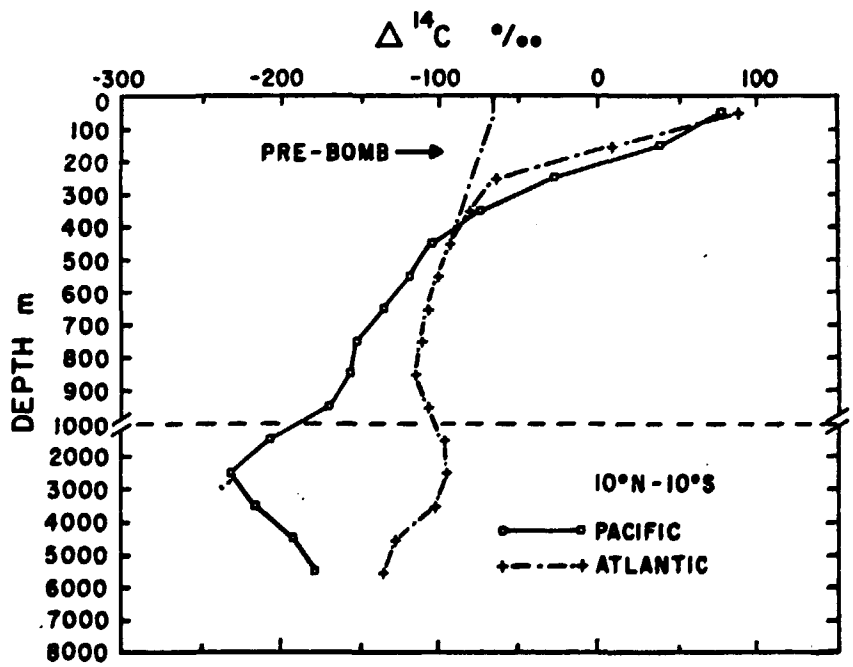

Fig. 4.1(b): $\Delta^{14}C$-depth profiles for the equatorial (10°N-10°S) regions of the Atlantic and Pacific Ocean. The assumed pre-bomb depth profile extends to a $\Delta^{14}C$ surface value of $-65‰$. (Taken from Stuiver et al. [1981]).

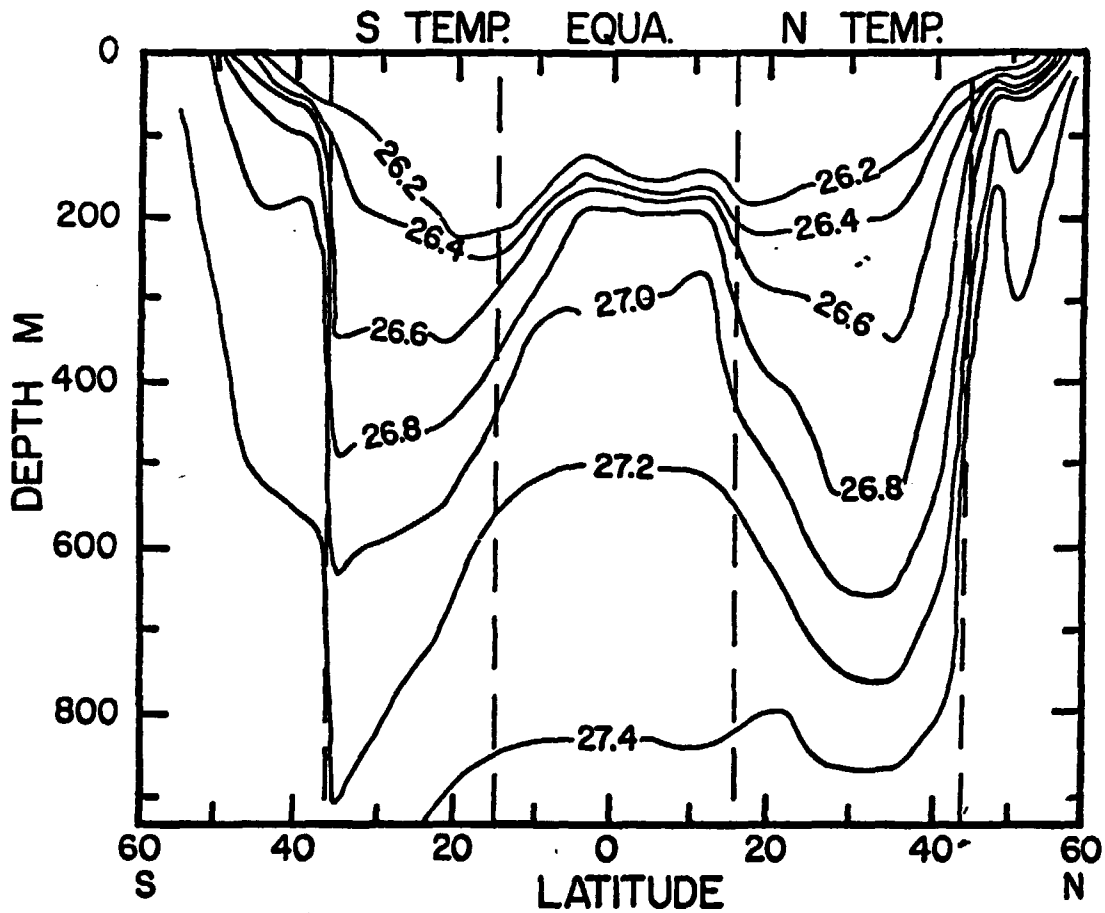

Fig. 4.2: Density versus depth along the western Atlantic GEOSECS track. The dashed lines separate the deep temperature thermocline from the shallow equatorial thermocline. The density unts are per mil deviation from 1 kg/l. (Taken from Broecker and Peng, [1981].

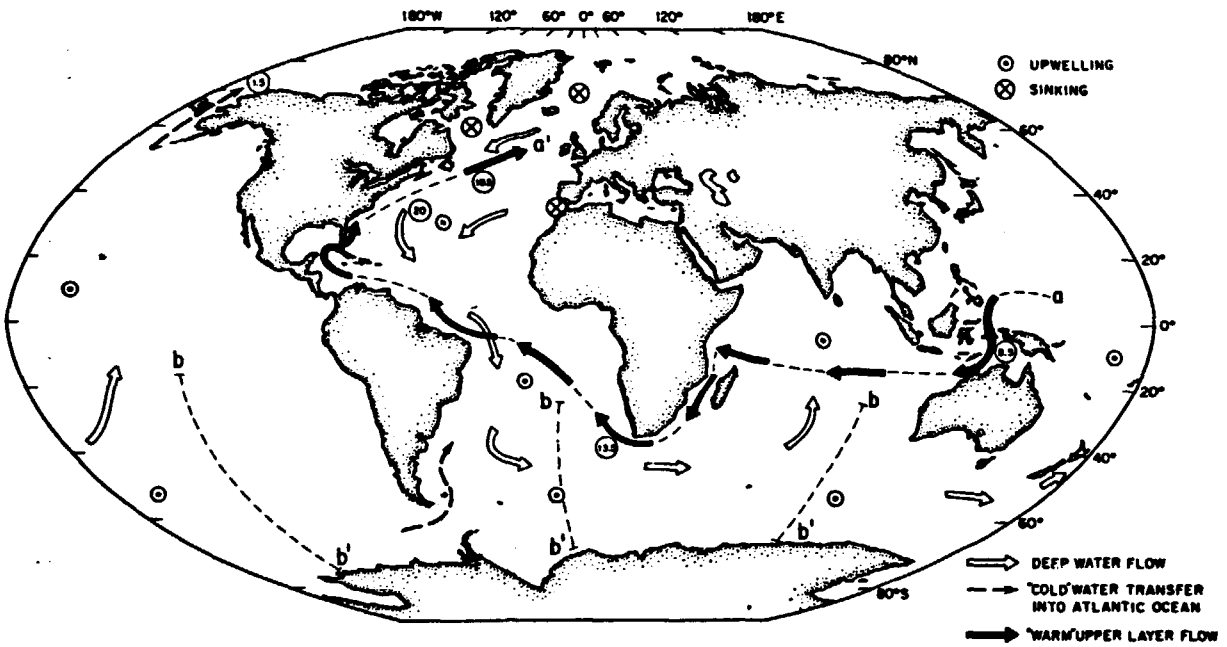

Fig. 4.3(a): Global structure of the thermohaline circulation cell associated with NADW production. The warm water route, shown by the solid arrows, marks the proposed path for return of upper layer water to the northern North Atlantic as is required to maintain continuity with the formation and export of NADW. The circled values are volume flux in 10^6 m^3/s which are expected for uniform upwelling of NADW with a production rate of 20×10^6 m^3/s. These values assume that the return within the cold water route, via the Drake Passage, is of minor significance. (NADW = North Atlantic Deep Water.) (Taken from Gordon [1986]).

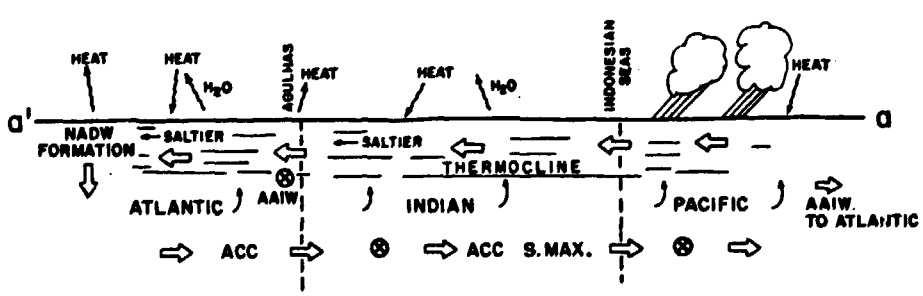

Fig. 4.3(b): Schematic representation of the thermohaline circulation cell associated with NADW production and the warm water route along line a-a' shown in Figure 4.3(a). The upper layer water within the main thermocline begins its passage to the North Atlantic in the Pacific as low-salinity water. It enters the Indian Ocean via the Indonesian seas, where its salinity and volume flux increase by excess evaporation and further upwelling of NADW, respectively. The thermocline water enters the Atlantic south of Africa and spreads to the northern Atlantic, continuing to increase in salinity and volume flux (from Gordon [1986]).

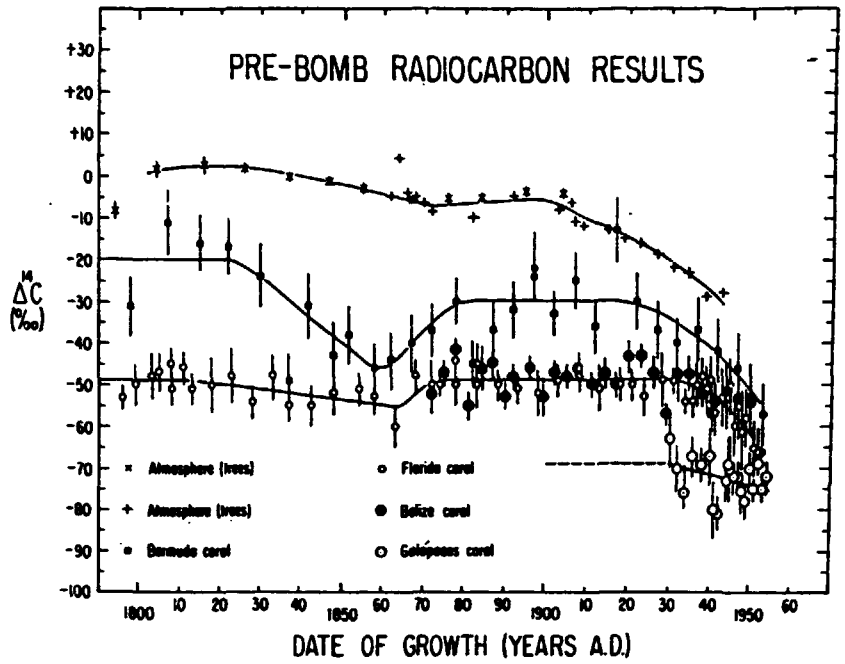

Fig. 4.4(a): Radiocarbon measurements for corals and tree rings that grew during the period A.D. 1800-1952. The trees were collected from the Pacific Northwest in the United States and from the Netherlands. The corals were collected from Florida and Belize [Druffel and Linick, 1978; Druffel, 1980], from the Galapagos [Druffel, 1981] and from Bermuda [Nozaki et al., 1978]. (Taken from Druffel and Suess [1983]).

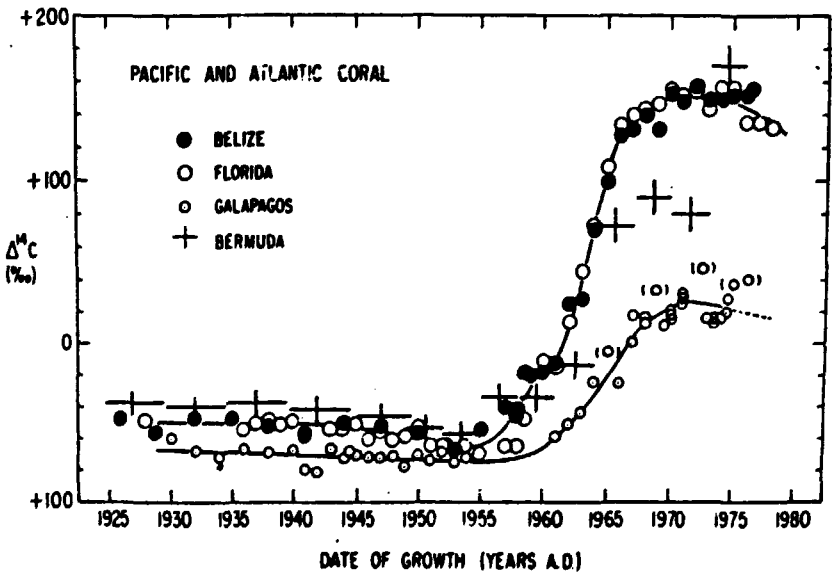

Fig. 4.4(b): Radiocarbon measurements for the corals of fig. 4.4(a) growing from 1925 to 1978. A considerable difference is noticed among the coral locations. This is attributed to the source of surface waters for each location. (Taken from Druffel and Suess [1983]).

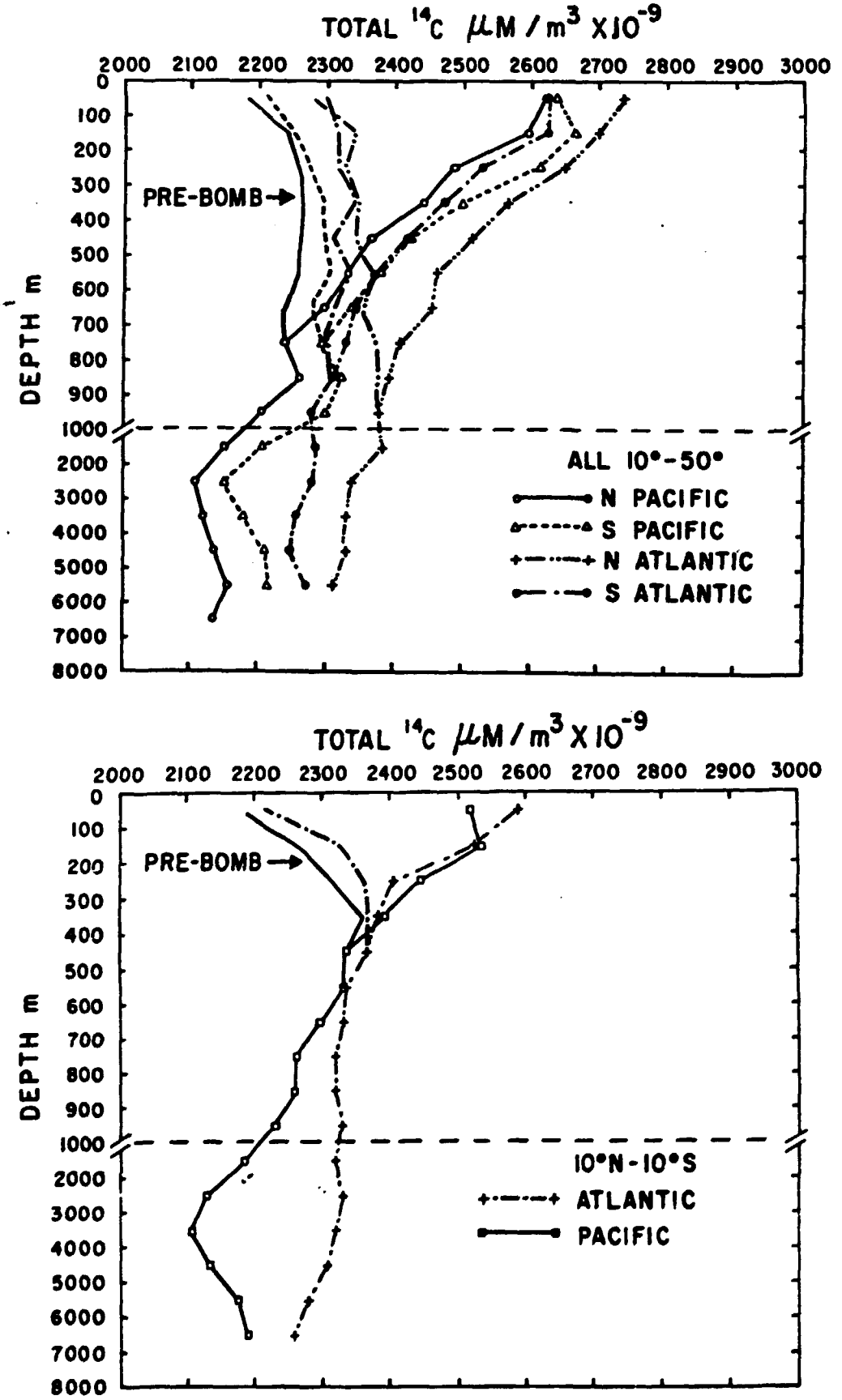

Fig. 4.5: Dissolved inorganic ^{14}C versus depth corresponding to the profiles of fig. 4.1. Note that 2000×10^{-9} $\mu M/m^3$ is equivalent to 1.2×10^9 atoms $(^{14}C)/l$. (Taken from Stuiver et al. [1981]).

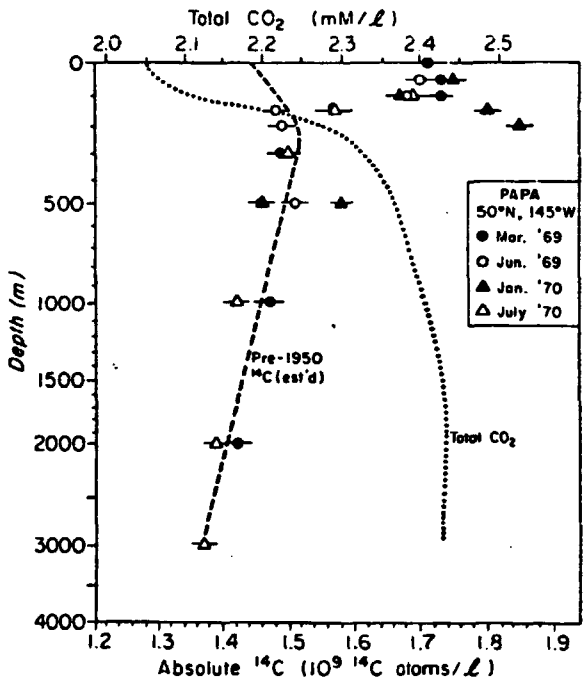

Fig. 4.6(a): ^{14}C concentrations at the North Pacific weather station PAPA. The dotted line gives the total DIOC profile ("Total CO_2"). The dashed line is the estimated natural ^{14}C level. (Taken from Fairhall et al. [1972].

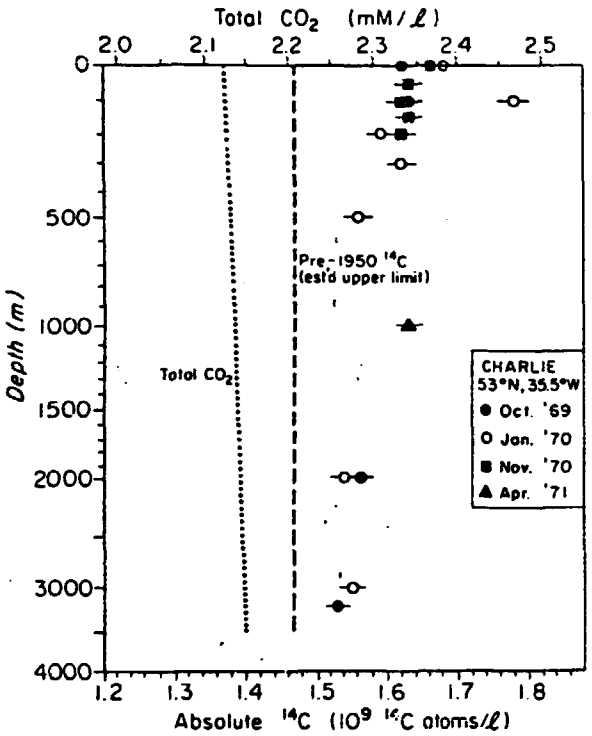

Fig. 4.6(b): As for (a), but for the North Atlantic weather station CHARLIE.

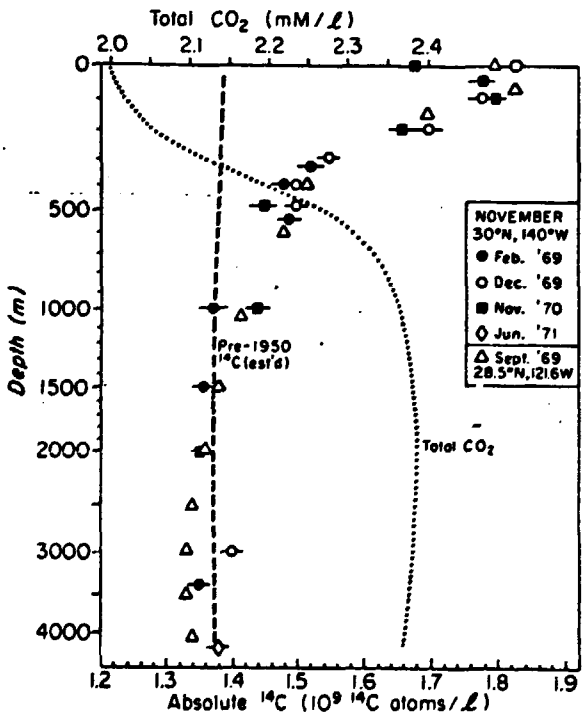

Fig. 4.6(c): As for (a), but for the mid-Pacific Ocean weather station NOVEMBER. Open triangles are data from the GEOSECS station.

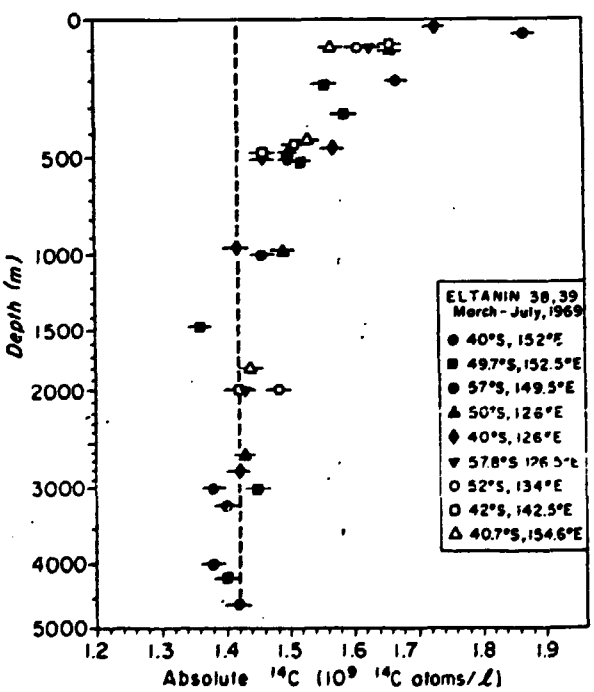

Fig. 4.6(d): As for (a), but for the ocean south of Australia in mid-1969.

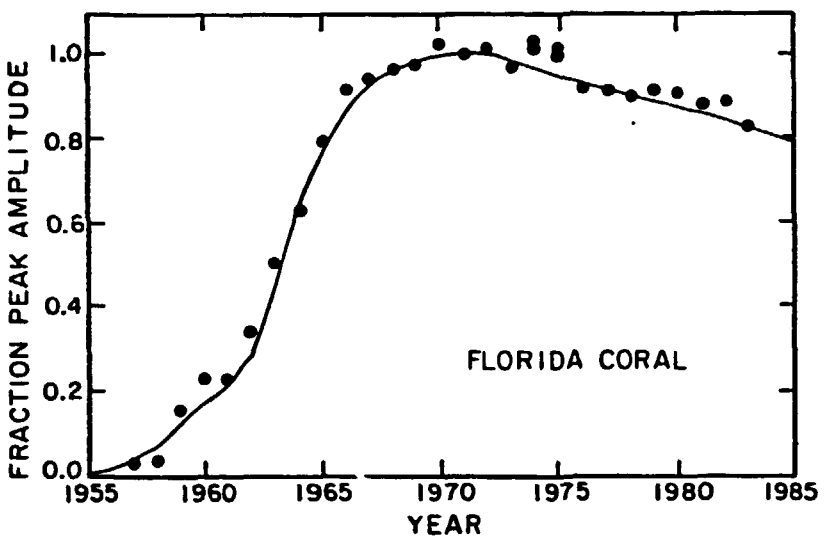

Fig. 4.7(a): The atmospheric radiocarbon histories in three latitude zones used to assess CO_2 invasion. These curves are based on radiocarbon analyses for atmospheric CO_2 carried out mainly in the Trondheim, Norway, and Heidelberg, Germany, laboratores (Taken from Broecker et al. [1985]).

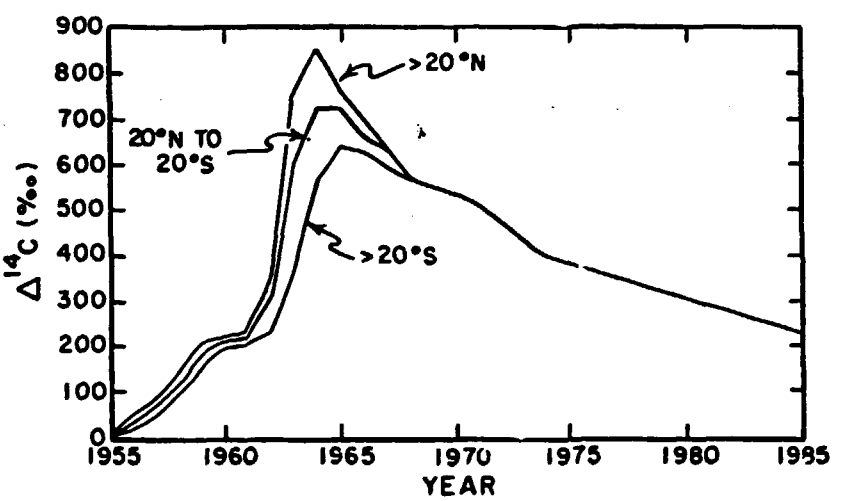

Fig. 4.7(b): The shape of $\Delta^{14}C^*$ versus time trend adopted by Broecker et al. [1985] for segregating the bomb and cosmogenic ^{14}C at all surface ocean sites. It is based on the ring-dated coral results of Druffel and Linick [1978] for the Florida Straits. (Taken from Broecker et al. [1985]).

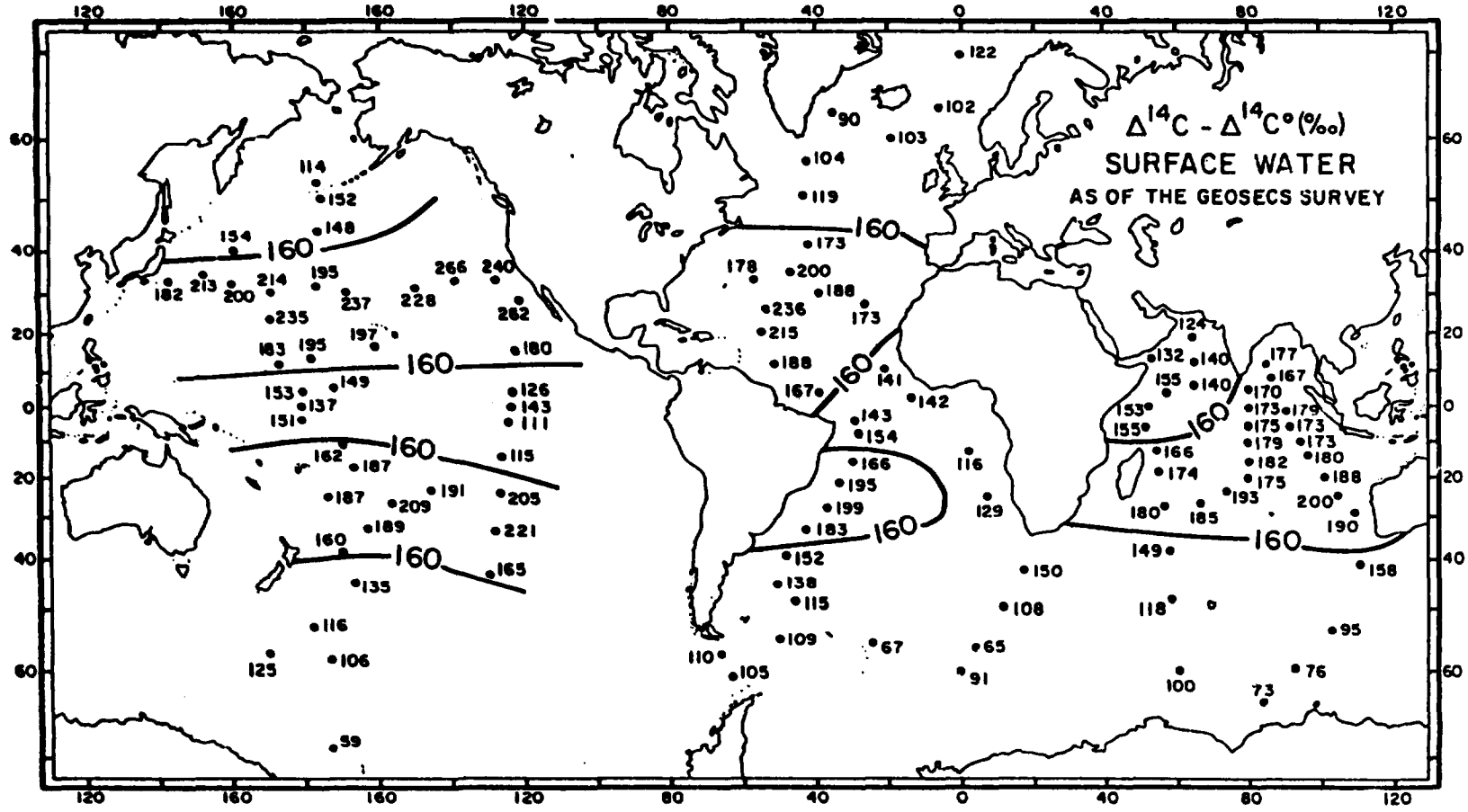

Fig. 4.8: Map showing the distribution of $\Delta^{14}C$ excesses (over the prenuclear values) for surface waters at the time of the GEOSECS surveys. (Taken from Broecker et al. [1985]).

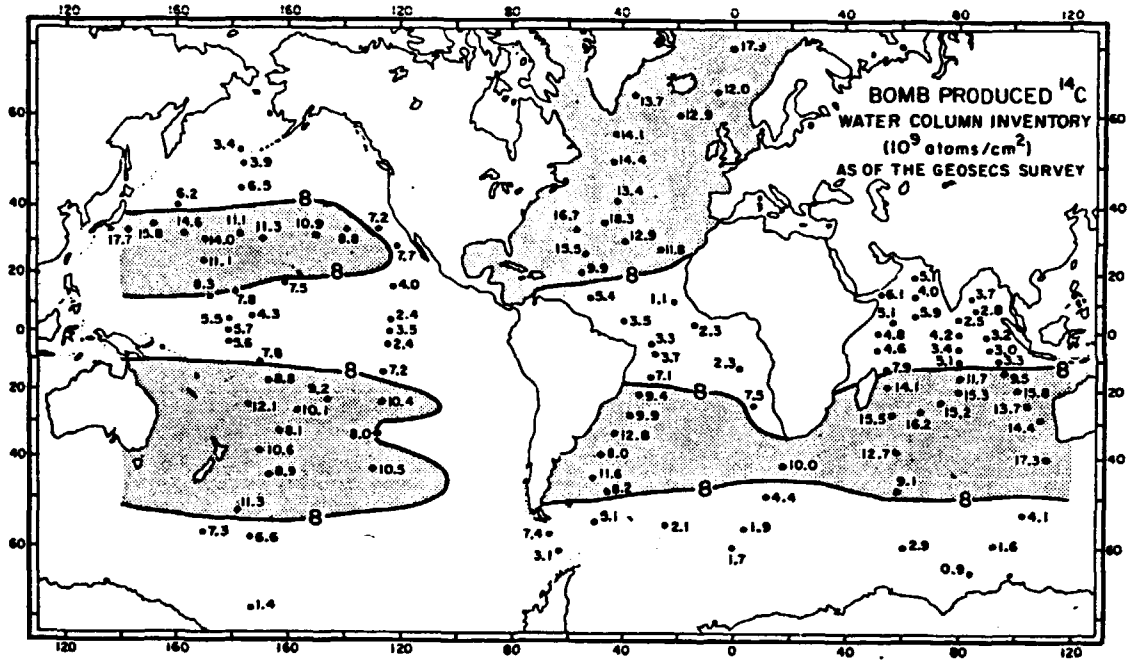

Fig. 4.9(a): Water column inventories for bomb radiocarbon at the stations occupied during the GEOSECS program. (Taken from Broecker et al. [1985]).

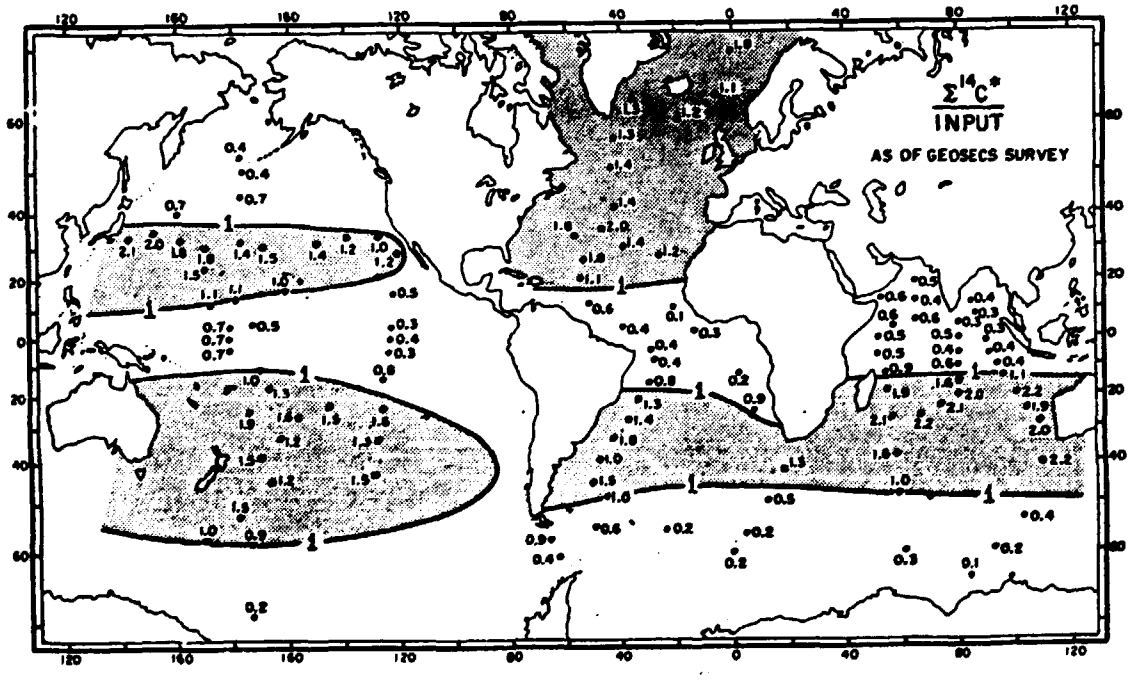

Fig. 4.9(b): Ratio of water column inventory to net input of bomb radiocarbon for the stations occupied during the GEOSECS program. The ratio averaged over each of the three main oceans is unity. (Taken from Broecker et al. [1985]).

5. RADIOCARBON EXCHANGE BETWEEN ATMOSPHERE AND OCEAN

With the oceans representing a thin wafer on the earth's surface (vertical:horizontal dimensions approximately $1:10^4$), the ocean-air interface plays an important role in both carbon balance and marine chemistry. The uppermost (mixed) layer of ocean, averaging some 75m in depth, contains about the same amount of carbon as does the overlying atmosphere, and yet has only about 1.8% of all oceanic carbon [Takahashi and Azevedo, 1982]. The fact that prevailing carbon excesses (both bomb-^{14}C and fossil fuels) have already substantially impacted upon the marine environment reflects the time scale (of about a decade or less) governing carbon exchange between atmosphere and surface ocean.

In this chapter we discuss the current state of knowledge of oceanic carbon dynamics, including the atmospheric source. This involves an overview of carbon chemistry, perceptions of the mechanisms of CO_2 exchange across the air-sea interface, and models of carbon cycling which attempt to integrate disparate parcels of information on carbon reservoirs and turnovers.

5.1 Oceanic Carbon Chemistry

Organically-bound carbon comprises a tiny fraction of oceanic carbon, but nevertheless plays an important role in carbon balance. It is thus useful to first consider carbonate cycles and relegate organic chemistry to a consideration of its complementary role. The review here is largely taken from the USDoE expert analysis by Baes et al. [1985], with some detail extracted from the book by Broecker and Peng [1982, p58ff, p149ff, p280ff].

DIOC denotes "dissolved inorganic carbon". Square braces enclosing a chemical entity denote its concentration. The partial pressure difference at the interface (ocean minus atmosphere) is denoted ΔpCO_2.

5.1.1 Carbonate chemistry

The dissolution of gaseous CO_2 in water forms (aqueous) carbonic acid according to the reversible reaction

$$H_2O + CO_2 \rightleftarrows H_2CO_3. \qquad (5.1)$$

The carbonic acid can dissociate into bicarbonate and carbonate ions:

$$H_2CO_3 \rightleftarrows H^+ + HCO_3^-, \qquad (5.2)$$

$$HCO_3^- \rightleftarrows H^+ + CO_3^{2-}. \qquad (5.3)$$

(Note that some writers refer to aqueous CO_2 rather than to carbonic acid, treating as an inert gas in solution which coexists with the

bicarbonate and carbonate ions). The extent of CO_2 dissolution is determined by the CO_2 partial pressure in the water (denoted pCO_2) - which equals that in the overlying air under equilibrium conditions - according to

$$[H_2CO_3] = K_1 \ (pCO_2) \tag{5.4}$$

where K_1 is termed the solubility of CO_2. The extent of carbonic acid dissociation is determined by the equilibrium constants K_2, K_3:

$$[HCO_3^-] \ [H^+] = K_2 \ [H_2CO_3], \tag{5.5}$$

$$[CO_3^{2-}] \ [H^+] = K_3 \ [HCO_3^-]. \tag{5.6}$$

The constants K_1-K_3, presumed to reflect aqueous equilibrium, depend upon salinity, pressure and temperature; Takashahi et al. [1976] have appraised the various catalogues of this dependency. Typically, K_1 = $4x10^{-2}$ mole/kg/atm, K_2 = $1.1x10^{-6}$ mole/kg, K_3 = $7x10^{-4}$ K_2in marine surface conditions at 15°C.

The [DIOC] of Chapter 4 is

$$[DIOC] = [H_2CO_3] + [HCO_3^-] + [CO_3^{2-}]. \tag{5.7}$$

Typical profiles of [DIOC] are displayed in fig 5.1 as well as in fig. 4.6. For a description of regional variations in [DIOC], see Takahashi and Azevedo [1982]. Table 5.1 records the estimated depth structure of the DIOC inventory.

An important oceanic store of inorganic carbon is calcium carbonate ($CaCO_3$). This material is prevalent in ocean sediments in two forms, calcite and the more soluble aragonite, and its dissolution provides a source of carbonate ions:

$$CaCO_3 \rightleftharpoons Ca^{2+} + CO_3^{2-}. \tag{5.8}$$

The saturation concentration for each species at equilibrium is governed by

$$K_4 = [Ca^{2+}] \ [CO_3^{2-}]; \tag{5.9}$$

K_4 has been recorded as a function of temperature, pressure and salinity. Of these, the monotonic increase of K_4 with pressure is the most important dependence, for it ensures that calcite raining from the

surface is all dissolved in deep waters. As a result of this, and the deep source of surface water (in the North Atlantic), surface waters are super-saturated in $CaCO_3$ and deep waters under-saturated. See Broecker and Peng [1982, p58ff] for details.

The skeletons and shells of many marine organisms are fabricated from the $CaCO_3$ which super-saturates the surface waters. Ultimately - after much surface recycling - the $CaCO_3$ rains downward as detritus to be redissolved at depth. This provides a mechanism for downward transferral of DIOC.

Table 5.2 shows the ionic balance (major contributors only) in sea water. The carbonate and bicarbonate contributions to total anion concentration are small and are determined by the requirement of charge neutrality. Their contributions are known as the total alkalinity of the water: the alkalinity is the imbalance in ionic charges of strong electrolytes which is balanced only by dissociated weak acids, such as carbonic, boric, phosphoric acids. Alkalinity, denoted [Alk], is expressed in "equivalents" (molarity weighted by ionic charge) per unit of water. Thus,

$$[Alk] = [Na^+] + [K^+] + 2[Mg^{2+}] + 2[Ca^{2+}] - [Cl^-] - [Br^-] - 2[SO_4^{2-}] - [NO_3^-] \quad (5.10a)$$

$$= [HCO_3^-] + 2[CO_3^{2-}]. \quad (5.10b)$$

Contributions to (5.10b) from minor constituents (e.g. $H_2BO_3^-$, HPO_4^{2-}, OH^-, H_3SiO_4) have been ignored. The alkalinity is directly measurable and provides a useful oceanic "tracer" [Fiadeiro, 1980; Takahashi et al., 1981]. Typical alkalinity profiles are displayed in fig 5.1.

The [DIOC] and [Alk] are invariably greater at depth than at the surface (see fig 5.1, and the next section). The ionic balance which determines the alkalinity is

$$H_2CO_3 + CO_3^{2-} \rightleftharpoons 2HCO_3^- \quad (5.11)$$

with equilibrium constant

$$K_5 = \frac{[HCO_3^-]^2}{[H_2CO_3][CO_3^{2-}]} = \frac{K_2}{K_3} \quad . \quad (5.12)$$

For more detail on the DIOC-alkalinity balance see Broecker and Peng [1982, p68].

Because most of the DIOC is in dissociated form, a small fractional change in pCO_2 is not accompanied by the same fractional change in [DIOC]. This buffering is described by the "Revelle factor",

$$\beta = \frac{\partial \ln(pCO_2)}{\partial \ln[DIOC]}, \qquad (5.13)$$

evaluated at constant temperature, salinity and alkalinity for surface waters. This factor varies with oceanic parameters, ranging from 8 in warm waters to 15 in polar waters, and averaging about 10 [Takahashi and Azevedo, 1982]. As [DIOC] increases so β increases and the oceans' ability to absorb excess CO_2 diminishes. A derivative similar to (5.13), but with respect to [Alk] at constant [DIOC], is of similar magnitude to β but of opposite sign.

Nett CO_2 exchange depends upon ΔpCO_2 and therefore upon pCO_2 in surface waters (since atmospheric circulation homogenenises CO_2 partial pressures there); pCO_2 itself depends not only upon temperature (approximately 4% per °C) but also upon [DIOC] and [Alk]. This favours a nett eflux of CO_2 in regions of upwelling (particularly tropical waters) and nett influx in the downwelling gyre regions. Takahashi and Azevedo [1982] have mapped contours of ΔpCO_2, which map is reproduced by Baes et al. [1985]. Smethie et al. [1985] have measured ΔpCO_2 in the tropical North Atlantic (to latitude 15°N), noting that ΔpCO_2 is positive equatorward of about 10° and negative north of that latitude.

5.1.2 Organic chemistry affecting carbon balance

It is apparent from fig 5.1 that both [DIOC] and [Alk] are relatively depleted at the surface (by about 10% and 4%, respectively). This depletion is significant in its effect upon pCO_2 and therefore upon CO_2 exchange with the atmosphere. Its origin is in biological activity.

Surface oceans are deficient in nutrients (indeed, are near phosphorus-free) and relatively rich in dissolved oxygen. These features together with depleted DIOC are a result of photosynthetic processes which consume dissolved CO_2 and nutrients and produce oxygen. Such processes deplete DIOC but increase alkalinity. The precipitation of $CaCO_3$ to produce shells and skeletons depletes both DIOC and alkalinity, more than offsetting the photosynthetic increase in the latter.

Conversely, at depth (typically 1km) [DIOC] and [Alk] are augmented by the reverse processes: $CaCO_3$ dissolution and [DIOC] production by oxidation of organic debris. Nutrients (phosphate and nitrate) are coproduced by this oxidation at depth, consistently with observed profiles.

Baes et al. [1985] review estimates of the downward flux of organic carbon necessary to account for the export of DIOC and alkalinity from the surface. To within a factor of 5 the flux is 8 Gt(C) per annum or 2 mole/yr/m^2 of ocean surface. This compares well with the flux estimated by Fairhall as necessary to maintain a constant ^{14}C concentration (see section 4.3.4). It is also in accord with flux estimates of Suess [1980], who noted a correlation between flux and depth which suggested that organic carbon was recycled many times (especially at thermocline depths) before settling as faecal debris.

5.2 Concepts of Atmosphere-Ocean CO_2 Exchange

The flux of CO_2 invading the ocean surface is proportional to the partial pressure of atmospheric CO_2; similarly the evading flux is proportional to pCO_2. These opposing fluxes (also called the invasion and evasion rates) are denoted I and E. But what are the mechanisms by which CO_2 traverses the air-sea interface? At least two conceptual models have been put forward as contending descriptors of such gas exchange. The "stagnant film model" and "film replacement model" are discussed below. A more detailed description of each with quantitative support is supplied by Broecker and Peng [1982, p113ff]. An intercomparison of contending models (with their ancestry) is presented by Holmen and Liss [1984].

5.2.1 Stagnant film model

Gas transfer across an air-sea interface is presumed to be limited by molecular diffusion. Since diffusion in the gaseous medium far exceeds that in the aqueous medium (by a factor $\sim 10^4$), the limiting step is diffusion across the uppermost millimetre or less of sea surface.

The stagnant film model (SFM) idealises the diffusive transfer by considering a thin film (thickness z) of sea at the interface between two well-mixed reservoirs of gas, each of uniform concentration (and partial pressure). The concentrations at the film boundaries are in equilibrium with the respective reservoirs, and across the film is a constant concentration gradient; the partial pressure is thus continuous across the interface.

The "film" is of course a hypothetical concept, being merely the thickness of water across which the diffusing gas would experience the necessary differential in partial pressure. An artifact is the sharp change in concentration gradient at the film-sea boundary. For an extensive discussion see Broecker and Peng [1974; 1982, p113ff].

According to the SFM the invasion and evasion rates are

$$I = pK_1 D/z, \qquad E = C_0 D/z, \tag{5.14}$$

where: D is the molecular diffusivity of the gas in sea water, C_0 is its aqueous concentration in the mixed layer, p is its atmospheric partial pressure; K_1 is its solubility at partial pressure p. Thus pK_1 is the aqueous concentration of the gas in equilibrium with the prevailing atmosphere (see equn (5.4)). The model depends only upon the ratio D/z, termed the piston velocity or transfer velocity of the gas. In principle, D is independently measureable for different gases and temperatures (e.g. see Broecker and Peng [1982, Table 3-3]), and the film-thickness might be expected to be gas-independent.

For a gas such as CO_2 which reacts chemically with water, C_0 of equn (5.14) measures the concentration of unreacted gas (undissociated H_2CO_3 in the case of CO_2 transfer). Thus the dissociative reactions consume or generate aqueous CO_2; Bolin [1960] was apparantly the first to

account for this hydration in applying the SFM to oceanic CO_2, though in a manner subsequently shown to require correction [Quinn and Otto, 1971].

The tacit assumption of the SFM is that z is gas-independent (though dependent upon climatic parameters such as temperature, wind speed), or, equivalently, that piston velocity is proportional to D. Consequently, W.S. Broecker, T.-H. Peng and co-workers have developed a novel means of assessing CO_2 exchange fluxes by utilising measurements of dissolved radon gas (radioisotope ^{222}Rn with half-life 3.8 day, a daughter of ^{226}Ra indigenous to all marine waters); they call this the "radon method" [Broecker et al., 1967; Broecker and Peng, 1971; Peng et al., 1974, 1979; Broecker and Peng, 1982, p122ff].

The idea of the radon method is that for seas not severly disturbed over the radon lifetime (about 6 day), Rn concentrations reflect equilibrium with the parent. The exception is near the surface (typically throughout the mixed layer and upper thermocline) where Rn concentration is deficient due to its evasion into the overlying air (usually devoid of Rn). The deficit can be determined from Ra and Rn profiles, and the SFM used to infer the equivalent film thickness. This thickness can be used in conjunction with CO_2 diffusivities to estimate CO_2 exchange rates. Some such estimates are:

- in the BOMEX area (tropical Atlantic, 15°N, 56°W), D/z = 700 m/yr = 2 m/day for Rn corresponding to z = 62 μm, from which E = 9.8 mole (CO_2)/yr/m^2 [Broecker and Peng, 1971];
- at station PAPA (windy North Pacific, 55°N, 145°W), D/z = 3.6 m/day for Rn corresponding to z = 20 μm [Peng et al.,1974];
- as a global mean based on GEOSECS Atlantic and Pacific data, D/z = 2.9 m/day for Rn corresponding to z = 36 μm, from which E = 16±4 mole (CO_2)/yr/m^2 [Peng et al., 1979].

Broecker and Peng [1974] list values of z for radon evasion at 31 West Atlantic GEOSECS stations between 69°N and 55°S; z ranges from 26 μm to 126 μm. A histogram of radon film thicknesses in different latitude bands is reported as fig 5.2 where a tendency for thicker films in equatorial regions is noted. Smethie et al. [1985] catalogue recent (TTO) values for D/z and z, calculated by the radon method.

Stuiver [1980a] analysed radiocarbon data from GEOSECS Atlantic stations, and deduced CO_2 exchange rates from which film thicknesses z are inferred. The latter ranged from 12-66 μm, averaging 19 μm (which corresponds to E = 27.0 mole/yr/m^2) for the western Atlantic; and from 15-138 μm, averaging 28 μm (E = 18.7 mole/yr/m^2) for the eastern Atlantic. These estimates of z do not employ the radon method, and seem systematically smaller that the radon-deduced z.

Broecker et al. [1980c] list CO_2 evasion rates calculated using the radon method as well as from bomb-^{14}C and cosmogenic-^{14}C distributions. Whilst agreement is favourable, radon-method evasion rates tend to be smaller. This is attributed either (a) to inadequacies in the SFM, and/or (b) on the basis of the short residency times for radon in the

mixed layer compared to the many years for CO_2 including periods of inclement weather. The latter is pertinent because I and E increase significantly with wind speed (perhaps with its square).

5.2.2 Film replacement and other models

There are several alternatives to the SFM of gas transfer, and of these the film replacement model (FRM) has a 50-yr history (mainly in the engineering literature); for a summary of its lineage, see Holmen and Liss [1984] and/or Smethie et al. [1985]. As with the SFM this model envisions molecular diffusion through a film of sea as the rate-limiting process. According to the FRM the film of surface water is periodically replaced by water from the interior which bring with it the properties of the bulk liquid. The rate-determining parameter is the film replacement time, analogous to the SFM's film thickness. The main empirical distinction between the SFM and FRM is that the piston velocities are proportional to D and to $D^{1/2}$ respectively (D being the molecular diffusivity).

Holmen and Liss [1984] assumed a piston velocity proportional to D^n and sought an optimal value for n to fit data from their laboratory-tank experiments. They deduced that $n=0.57\pm0.15$, which would support the FRM and appear to rule out the SFM.

Smethie et al. [1985] discussed models of gas exchange, noting that the Holmen and Liss result did not preclude $n=2/3$. This exponent is predicted semi-empirically by Deacon [1977] who adopted boundary-layer theory used with success for turbulent flow over a smooth wall. Smethie et al. presumed a $D^{1/2}$ dependence to estimate CO_2 fluxes from radon-evasion data; these fluxes were compared with those given by the "radon method" (with piston velocity linearly dependent upon D). Both piston velocities and nett CO_2 fluxes are smaller with the $D^{1/2}$ assumption.

5.3 Radiocarbon Balance and the CO_2 Exchange Rate

The dominant source of $DIO^{14}C$ is atmospheric, and the dominant sink is by radioactive decay (mean life, $\lambda^{-1} = 8267$ yr). This section discusses the balance between the two, particularly in the light of perturbing injections of bomb-carbon into the atmosphere.

The term "exchange rate" refers to either an invasion or evasion rate. In a global steady state nett exchange is nil and the term therefore unambiguous.

Local exchange rates are expected to be proportional to the partial pressure in the departing medium. Thus, pre-industrial rates ($pCO_2 \approx$ 290 μatm) would be less than modern rates ($pCO_2 \approx 340$ μatm). Baes et al. [1985, p92] therefore deem it appropriate to cite exchange rates per unit partial pressure (e.g. mole/yr/m^2/μatm).

5.3.1 Equilibrium in the pre-bomb era

If one assumes a pre-industrial steady state distribution of ^{14}C, a back-of-envelope calculation can indicate the invading CO_2 flux from the atmosphere necessary to maintain this equilibrium.

Assume a pre-industrial oceanic inventory of 1.96×10^{30} atoms (^{14}C) (table 4.3), of which a fraction 1/8267 decay every year - a radioactive loss of 6.6×10^{11} atoms/yr/m^2 of ocean surface. At steady state the average exchanging CO_2 fluxes (I and E) exactly cancel, but because of an imbalance in $^{14}C/^{12}C$ ratio there is a nett air-to-sea ^{14}C flux of

$$1.176 \times 10^{-12} \times 1.052 \times 10^{-3} \times \{\Delta^{14}C(\text{air}) - \Delta^{14}C(\text{surface})\} \times E\ N_0,$$

where N_0 is Avagadro's number and E is in mole(CO_2)/yr/m^2. The factor 1.052 accounts for fractionation [Stuiver, 1980a]. Equating source and sink and setting interfacial $\Delta^{14}C$ increment at 45°/$_{oo}$ provides E = 19.7 mole/yr/m^2 (or 0.068 mole/yr/m^2/μatm). This can be expressed in terms of the average residence time for atmospheric CO_2 with respect to oceanic invasion: this time is N/AE, where N is the atmospheric CO_2 inventory in mole and A is the ocean surface area. For E = 19.7 mole/yr/m^2 and $N = 51 \times 10^{15}$ mole [Bolin et al., 1981], the residence time is 7.2 yr. The major uncertainty in this estimate is in the $\Delta^{14}C$ increment at the air-sea interface.

Similar "back-of-envelope" calculations have been performed by Peng et al. [1979], by Broecker et al. [1979] and by Bolin et al. [1981], among others, each with different numerical input. The three estimates of E are near 19 mole/yr/m^2, with about 25% uncertainty.

More detailed fluxes (regional dependences etc) are no longer amenable to estimation based on pre-nuclear radiocarbon distributions; the requisite data base is not available. Such detail is available from the ongoing redistribution of bomb carbon.

5.3.2 Response of the bomb-carbon signal

The invading bomb carbon provides a rare opportunity to study the dynamics of CO_2 exchange at the ocean-air interface. This opportunity has two caveats. First, time-series data of the invasion is not available, save one exception, because extensive surveys have yet to follow up GEOSECS. The exception is the excellent data documented by Nydal et al. [1984], so far incompletely analysed. The second caveat is the caution by Broecker et al. [1980b] that equilibration times for isotopes of carbon are longer by an order of magnitude than CO_2 residence times in the surface ocean and atmosphere. Hence the distribution of DIO^{14}C among the chemical species in the ocean (bicarbonate and carbonate ions) may not mirror the distribution of DIOC. Such a consideration would affect estimated evasion rates more than invasion rates, and even then not in the pre-1972 era when $\Delta^{14}C$ values were much larger in the atmosphere.

Some exchange rate estimates from bomb-carbon distributions are outlined below; others deduced by the radon method are reported in section 5.2.1.

(a) Munnich and Roether [1967]:

This early calculation based on a 1965 Atlantic survey assumes that bomb-carbon and tritium have penetrated to the same depths. An average CO_2 piston velocity of 2.1 km/yr (5.8 m/day) is indicated, corresponding to an exchange rate of 23 mole/yr/m^2.

(b) Stuiver [1973]:

Stuiver summarises existing estimates of atmospheric residence times based on early bomb-carbon data. These lie in the range 4 to 10 yrs, with a further value of 25 yr (an estimate by Bien and Suess [1967]) computed with respect to a terrestrial rather than oceanic sink.

(c) Stuiver [1980a]:

The GEOSECS Atlantic results are analysed separately for the eastern and western Atlantic. The bomb component $\Delta^{14}C^*$ is segregated from measured values by assuming a pre-industrial surface value $-40^o/_{oo}$ and an equal penetration of bomb carbon and tritium. By assuming that the bomb-carbon column inventories are derived solely from the overlying air of known history (i.e. none is by lateral advection), an exchange rate can be estimated. The average exchange rate for the western and eastern Atlantic is 27.0 and 18.7 mole/yr/m^2, with an Atlantic average of 23 mole/yr/m^2. For a typical 1960's atmospheric inventory of 57×10^{15} mole (CO_2), or 158 mole/m^2 of ocean surface, the mean atmospheric residence time is 158/23 = 6.8 yr.

(d) Quay and Stuiver [1980]:

Quay and Stuiver put forward a model of vertical transport to intepret GEOSECS data in and overlying the thermocline. Bomb carbon invades the sea surface and is mixed by vertical advection and diffusion. The CO_2 exchange rate matches input to inventory; the area-weighted rate for the Atlantic is then 21 mole/yr/m^2, and that for the Pacific (with sparser data) is about 25 mole/yr/m^2. However, unlike the Atlantic, the Pacific bomb-carbon distribution is not well explained by vertical transport alone.

(e) Stuiver *et al.* [1981]:

Mid-Atlantic and mid-Pacific GEOSECS results are given preliminary analysis (see section 4.3.3). Average exchange rates in the tropical and gyre regions are estimated as in Stuiver [1980a] above; the resulting rates are reported in table 4.1.

(f) Broecker *et al.* [1985]:

Broecker *et al.* deduce ocean-average CO_2 exchange rates separately for the Atlantic, Pacific and Indian Oceans of 22.3, 19.4 and 19.2 mole/yr/m^2; see section 4.3.5 for details. The area-weighted average for world oceans is 20.1 mole/yr/m^2 which, by design, matches the bomb-carbon inventory to assumulated input. The temperate regions together with the North Atlantic show an inventory excess over apportioned input (fig 4.9b). This is explainable in part by local exchange rates

depending upon average wind speeds. For reported wind speed dependences, Broecker et al. assessed that invasion rates would be reduced to about 0.7 and 0.9 of global means in the tropical and north temperate zones, and enhanced by a factor of about 1.1 and 1.3 in the south temperate and high-latitude zones. This partly explains the "Inventory-Input" variations in table 4.2b. Table 5.3 reports the reassessed wind-corrected invasion rates for the latitude bands in table 4.2b.

(g) Smethie et al. [1985]:

Smethie et al. report extensive winter measurements of pCO_2 and of radon profiles in the tropical Atlantic surface (the TTO survey). The piston velocities, estimated by the radon method, increase with wind speed. The differential in CO_2 partial pressure at the sea-air interface (ΔpCO_2) vary between -35 μatm and 64 μatm, with null value at near 10°N. North of this latitude the nett CO_2 flux into the ocean peaked at 1.4 mole/yr/m^2 (at 15°N), and the tropical peak outflow was 2.7 mole/yr/m^2 at 8°S. The separate invading and evading fluxes were not estimated.

5.3.3 Sources of CO_2-exchange variation

Nett CO_2 fluxes from atmosphere to ocean are known to depend upon marine conditions (temperature, salinity, pCO_2) and upon the prevailing wind speed. The mechanism for the latter seems not to be well understood, conceptually or empirically. In laboratory experiments Kanwisher [1963] has deduced empirically an exchange rate varying with the square of wind speed; however such a dependence seems to be only roughly applicable to oceanic conditions [Broecker and Peng, 1974; Peng et al., 1979; Broecker et al., 1980c, Wannikhof et al., 1985; Smethie et al., 1985]. Within the context of the SFM (section 5.2.1) the effect of wind speed is to agitate the water and decrease the film thickness (or increase the piston velocity).

The magnitude of surface-water pCO_2 depends upon temperature, alkalinity and [DIOC]; the manner of these interdependences is outlined in section 5.1. For a detailed discussion see Takahashi and Azevedo [1982] and/or Smethie et al. [1985].

5.4 Models of the Global Carbon Cycle

It is unnecessary to undertake detailed carbon-cycle modelling in order to estimate radiocarbon inventories and dynamics in the oceans. However, it is useful to appraise the overall consistency of apportioned carbon and radiocarbon. Accordingly, only the main features and developments of global carbon models are mentioned, including their successes and shortcomings in respect of radiocarbon and oceanic DIOC.

5.4.1 Model structures

The major model developments are outlined below. For more detail, see the review by Emanuel et al. [1985].

(a) Few-box models:

The simplest models represent major carbon reservoirs by a small number of boxes in each of which the carbon is well mixed at all times. The kinematics are represented by flow rates between pairs of boxes. Craig [1957] considered a 5-box model (atmosphere, biosphere, humus, surface ocean, deep sea) from which he estimated turnover times. A similar 3-box structure of atmosphere and ocean was used by Rafter and O'Brien [1970] to interpret southern Pacific data. In all cases the deep-sea box communicates only with the surface ocean. These models generally do not well portray DIOC transfer to the deep ocean. Nevertheless, their simplicity remains their major asset; Bacastow and Keeling [1979] show that even such a 2-box ocean model is adequate if the box sizes are selected empirically - e.g. if the surface-ocean box represents the upper 260m (say) rather than the 75m usually associated with the mixed layer, thereby apportioning the thermocline between the two oceanic boxes.

(b) Box-diffusion models:

The so-called "Oeschger model" [Oeschger et al., 1975] has become the benchmark model for oceanic carbon transport - although some reparameterisations have been investigated [Siegenthaler and Oeschger, 1978; Broecker et al., 1978, 1980a]. The deep ocean is given vertical structure by means of a reservoir whose carbon is not well mixed but is continuously redistributed by unidimensional eddy diffusion. The Oeschger model has 5 reservoirs: atmosphere, long-term biosphere (with 60-yr lag), well-mixed surface ocean, eddy-diffusive deep ocean. The surface ocean is chosen as 75m deep (the accepted average depth of the mixed layer). Other parameters are selected to provide a best fit to the steady-state cosmogenic ^{14}C distribution: a vertical diffusivity $K = 1.26\ cm^2/s$ and exchange rates $k_{am} = 1/7.7$ and $k_{am} = 1/10$ yr for atmosphere-to-surface and surface-to-atmosphere, respectively. (For the assumed pre-industrial atmospheric inventory of 620 Gt(C), this value of k_{am} is equivalent to an invasion rate of $E = 18.6\ mole/yr/m^2$; contrast this with the values $E = 16$ and $21\ mole/yr/m^2$ which Broecker et al. [1979 and 1980a, respectively] assert that Oeschger's group have adopted). Diffusion-controlled deep mixing seems to introduce a superior simulation of DIOC distribution without sacrificing structural simplicity. Such diffusion is seen as an empirical mimic of carbon transport to depth rather than as a conceptual portrayal. Siegenthaler and Oeschger [1978] use the model to predict the response to fossil-fuel combustion; some predictions depend markedly upon assumed values for the Revelle factor (equn(5.13)) and for the poorly-known biospheric growth rate. Broecker et al. [1980a] propose a retuning of parameters and note that tritium-penetration data favour a larger diffusivity ($\sim 1.7\ cm^2/s$). Broecker et al. [1979] note that increasing the depth of the surface-ocean box can improve the model's fit to fossil-fuel data.

(c) Modified box-diffusion models:

Several investigators have modified the Oeschger model in attempts to inject more realism into its structure or to test if model shortcomings were responsible for imperfect simulations. Broecker et al. [1980a] and Hoffert et al. [1981] independently introduced vertical advection into the model, with separate upwelling and downwelling regions. Hoffert et al. also included effects of a marine biosphere.

Crane [1982] and Siegenthaler [1983] added boxes to represent polar regions which outcrop to make contact with the atmosphere.

(d) Multi-box models:

In numerically implementing box-diffusion models to study carbon dynamics, Oeschger found it appropriate to stratify the diffusive reservoir into a finite number (viz, 42) of layers. Several recent models have explicitly incorporated a multi-box structure with the boxes and transfer pathways designed to simulate real oceanic processes. Bjorkstrom [1979] designed a model with a "cold" and "warm" surface ocean, a stratified (2 layers) intermediate ocean simulating the thermocline, and a deep ocean stratified into 8 boxes. Enting and Pearson [1982, 1983] developed a similar but more complex compartmental structure. Some other variations are developed for comparative purposes (see succeeding section).

5.4.2 Model intercomparisons

As well as the excellent summary by Emanuel et al. [1985] of the carbon models mentioned above, two attempts to compare the merits of such models are useful. Both attempts [Bacastow and Bjorkstrom, 1981; Killough and Emanuel, 1981] select representative models and calibrate them consistently (so that differences in their simulations are truly indicative of differences in their structures); the calibration requires that the models reproduce the steady-state pre-industrial distribution of radiocarbon (as well as it is known). Both intercomparisons have as objective a study of model responses to fossil-fuel combustion scenarios. A summary of these intercomparisons follows; more detail is provided by Emanuel et al. [1985].

(a) Bacastow and Bjorkstrom [1981]:

Four types of oceanic models are compared: a 2-box model (2B), a box-diffusion model (BD), an advection diffusion model (AD), and a multi-box model (MB). The 2B, BD and MB models are essentially those of sections 5.4.1(a), (b) and (d); the AD model is an extension of the BD model in which a direct "pipeline" between the surface and a deep-ocean box beneath the diffusive reservoir admits an advective flow to balance upwelling. The interest was in comparing the models' forecasts for scenarios for fossil-fuel combustion (in particular the forecasted "airborne fraction" (AF) of combusted fossil fuel). The models predicting the highest AF are those with the smallest oceanic reservoirs which are coupled by rapid transfer rates to the atmosphere (a 2B model with 75m deep surface). Model AD forecasts a higher AF than does BD. Bacastow and Bjorkstrom favour a BD for near-term forecasts, but with a higher diffusivity than Oeschger originally proposed. For longer term forecasting a retuned BD model should be satisfactory; this would feature a deeper surface ocean (201m) and diffusivity $K = 1.437$ cm^2/s, selected to simulate deep ^{14}C. Apparently no comparative test is made of the models' response to bomb carbon.

(b) Killough and Emanuel [1981]:

Five unidimensional models are compared. Models 1a, 1b both represent the ocean by two boxes (as in section 5.4.1(a)); they differ

in the depth of ocean represented by the surface-ocean box: 75m as against 260m. Models 2,3a and 3b all have a surface ocean of 75m depth overlying a 10-layer intermediate ocean of 75-1000m in depth which in turn overlies a 7-layer stratified deep ocean. These three models all accomodate vertical advection. In model 2 all sub-surface layers have access to surface water (cold water sinking) and each has a return pipeline to the surface (upwelling). In models 3a, 3b the upwelling is via layer-to-layer transport, and model 3b represents downward sinking in the same way. For model calibration the cosmogenic ^{14}C data base discussed in section 4.3.6 was carefully assembled. The performances of the models in predicting uptake of excess (fossil fuel) CO_2 are compared. Model 1a takes up the least (18%), and models 3a, 3b the most (49%) by 1975; in reality about 55% is believed still airborne, with most of the rest in the oceans. The uptake of bomb carbon predicted by the models to 1975 is: 260, 340, 410, 430, 430 $x10^{26}$ atoms for model 1a, 2, 1b, 3a, 3b, respectively; the second seems in best accord with the 1972 inventories of table 4.3.

5.4.3 Model overview

Emanuel et al [1985] summarise the comparative investigations discussed in the preceding section from the viewpoint of understanding the fate of atmospheric CO_2. They suggest that the important features of a model which govern how quickly excess CO_2 is taken up by the oceans is the effective size of those reservoirs which are coupled with short time constants to the atmosphere. The important interplay between model structure and calibration is stressed. Diffusion can be entirely replaced by advective transport among stratified levels and, suitably calibrated, both can provide equally good accounts of steady state distributions. But responses on the different time scales can differ. Both the Baes et al. summary and the intercomparisons noted in the preceding section have the fossil-fuel problem in mind, and hence a response time of order 50 yr. It is not apparant that model response on this time scale necessarily reflects model responses to the sharp bomb carbon signal; however, the responses of the Killough and Emanuel models to both inputs are similar.

The CO_2 exchange rate is not pinned down by these analyses. There is a close coupling between that rate and parameters which describe the rate of transfer to the deep ocean. For example, both Oeschger et al. [1975] and Broecker et al. [1980a] demonstrate the coupling between the atmospheric exchange rate and the deep-ocean diffusivity. Thus it is not possible to specify an average exchange (or invasion) rate to better than 25% (typically, 19±5 mole/yr/m^2); for modelling applications its selection will be in tandem with those of other rate constants. The invasion rate should be expected to have increased by ~15% since the mid 19th century due to the increased atmospheric CO_2 content. Hence a pre-industrial invasion rate of 19 mole/yr/m^2 is equivalent to perhaps 22 mole/yr/m^2 for the modern atmosphere (i.e. to 0.065 mole/yr/$m^2/\mu atm$).

The evasion rate will have undergone a similar (but slightly retarded) increase due to the close coupling and comparable sizing of the exchanging reservoirs.

5.5 Post-1972 Bomb-Carbon Inventory : An Update

The bomb-carbon inventory of table 4.3 is as of 1972. Since that time atmospheric bomb carbon has continued to invade the oceans. We can estimate the post-1972 invasion in a manner similar to Stuiver [1980a].

The nett flux of bomb ^{14}C from air to surface ocean is

$$(1.176\times10^{-12})(1.052)(10^{-3}\{I\times\Delta^{14}C^*_{air} - E\times\Delta^{14}C^*_{surf}\}$$

mole/yr/m^2. The factor 1.052 is due to relating fractionation to a normalised value of $\delta^{13}C = -25^o/_{oo}$ [Stuiver, 1980a]. We assume that the globally-averaged invasion and evasion rates (I and E) balance each other. This incurs slight error in that each is increasing due to the increasing CO_2 partial pressures in the departing medium. To select a representative invasion rate, we update the area-weighted average 20.1 mole/yr/m^2 from the Broecker et al. analysis (section 5.3.2(f)): a 2.5% enhancement to I = E = 20.6 mole/yr/m^2 acknowledges the 5% increase in CO_2 partial pressures over 1972-85.

The cumulative nett input of ^{14}C to world oceans since 1972 is then

$$5.53\times10^{24}\int_{1972}^{1985}\{\Delta^{14}C^*_{air}(t) - \Delta^{14}C^*_{surf}(t)\}dt \text{ atoms.}$$

The integral over $\Delta^{14}C^*_{air}$ is determined by noting that the post-1972 atmospheric record (fig. 3.1) is closely (and universally) approximated by an exponential decline from $470^o/_{oo}$ at a rate of 6.1% p.a. This integral then equates to $4219^o/_{oo}$-yr (equivalent to a 1972-85 average $\Delta^{14}C^*_{air} = 325^o/_{oo}$).

Globally-averaged $\Delta^{14}C^*_{surf}$ values are more elusive. Broecker et al. [1985, Table 10] have reported regional averages deduced from measurements; area-weighting these provides a global average $\Delta^{14}C^*_{surf}$ (1972) = $157^o/_{oo}$. The coral record adopted by Broecker et al. (fig. 4.7(b)) shows surface $\Delta^{14}*C$ values decreasing almost linearly since 1972 to 80% of that 1972 value by 1985. Accepting such a linear decline, the time-integral over $\Delta^{14}C^*_{surf}(t)$ is $1840^o/_{oo}$-yr (equivalent to an average value of $141^o/_{oo}$).

The cumulative nett input of ^{14}C during 1972-85 is thus 132×10^{26} atoms. Thus, supplementing the 1972 estimated inventory (table 4.3) the bomb-carbon inventory in the oceans as of 1985 is estimated to be 435×10^{26} atoms.

It is of interest to check the atmospheric inventory change for consistency. Inventories are cited in units of 10^{26} atoms. It is immediately clear from fig. 3.1 and table 3.1 that estimates of total atmospheric (tropospheric + stratospheric) inventory require extrapolation of the pre-1969 stratospheric estimates. At best, such extra-

plation can be guided by model forecasts. At worst it is complicated by the slow intra-stratospheric mixing which means that even the pre-1969 measurements on which table 3.1 is based may not typify the entire stratosphere (see section 3.3). Thus the atmospheric inventories of Levin et al. [1985] and Manning et al. [1986] reported in table 3.1 are subject to perhaps 25% uncertainty, and are more likely to be underestimates than overestimates. The 1972-1985 inventory decline is thus 101±25 units. Such uncertainty remains small compared with the cosmogenic inventory of 400 units.

Atmospheric input during 1972-1985 consisted of 9 units from nuclear detonations (at 1.2 units per Mt yield). The nett atmospheric exodus during this period was thus 110±25 units of bomb ^{14}C; this should be compared with the estimated nett input of 132 units to the oceans, leaving an atmospheric input of 22±25 units unaccounted for. Part of this discrepancy is due to exchange with the terrestial biosphere. While the magnitude of such exchange (even its sign) has not been reported, we note that Broecker et al. [1980] estimated bomb-^{14}C inventories for 1965 and 1969 in the various reservoirs and that these inventories required a nett eflux from biosphere to atmosphere. A continuation of this trend is concordant with the above estimates for 1972-1985.

Table 5.1

Oceanic inventory of DIOC*

Depth range (m)	[DIOC] m.mole/kg	Inventory 10^{15} mole (C)
0-50	2.012	37
50-1200	2.181	923
>1200	2.284	2206
whole ocean	2.254	3167

*Table adapted from Takahashi and Azevedo [1982]

Table 5.2

Charge balance in sea water: the excess cation charge is balanced by the dissociation of carbonic acid (H_2CO_3) into bicarbonate (HCO_3^-) and carbonate (CO_3^{2-}) ions. *

Positive			Negative		
Cation	Mass moles/kg	Charge eq/kg	Anion	Mass moles/kg	Charge eq/kg
Na^+	0.470	0.470	Cl^-	0.547	0.547
K^+	0.010	0.010	SO_4^{2-}	0.028	0.056
Mg^{++}	0.053	0.106	Br^-	0.001	0.001
Ca^{++}	0.010	0.020			
Total	-	0.606	Subtotal	-	0.604
			HCO_3^- + CO_3^{2-}	-	0.002
			Total	-	0.606

*Table taken from Broecker and Peng [1982, p.64].

Table 5.3

Regional invasion rates corrected for average wind speeds*

Region #	Invasion Rate (mole/yr/m^2)	Inventory/Input+
Atlantic Ocean	22.3	1.0
Northern	26	1.0
N. temperate	17	1.9
Tropical	15	0.6
S. temperate	22	1.2
Antarctic	≈26	0.3
Indian Ocean	19.4	1.0
Tropical	13	0.9
S. temperate	22	1.8
Antarctic	≈26	0.5
Pacific Ocean	19.2	1.0
Northern	23	0.5
N. temperate	19	1.4
Tropical	14	0.9
S. temperate	22	1.3
Antarctic	≈26	0.5

* Table from Brocker et al. [1985]

\# The latitude bands are those of table 4.2b

\+ The inventories are those of table 4.2b; the inputs are recalculated from table 4.2b using a wind-corrected invasion rate.

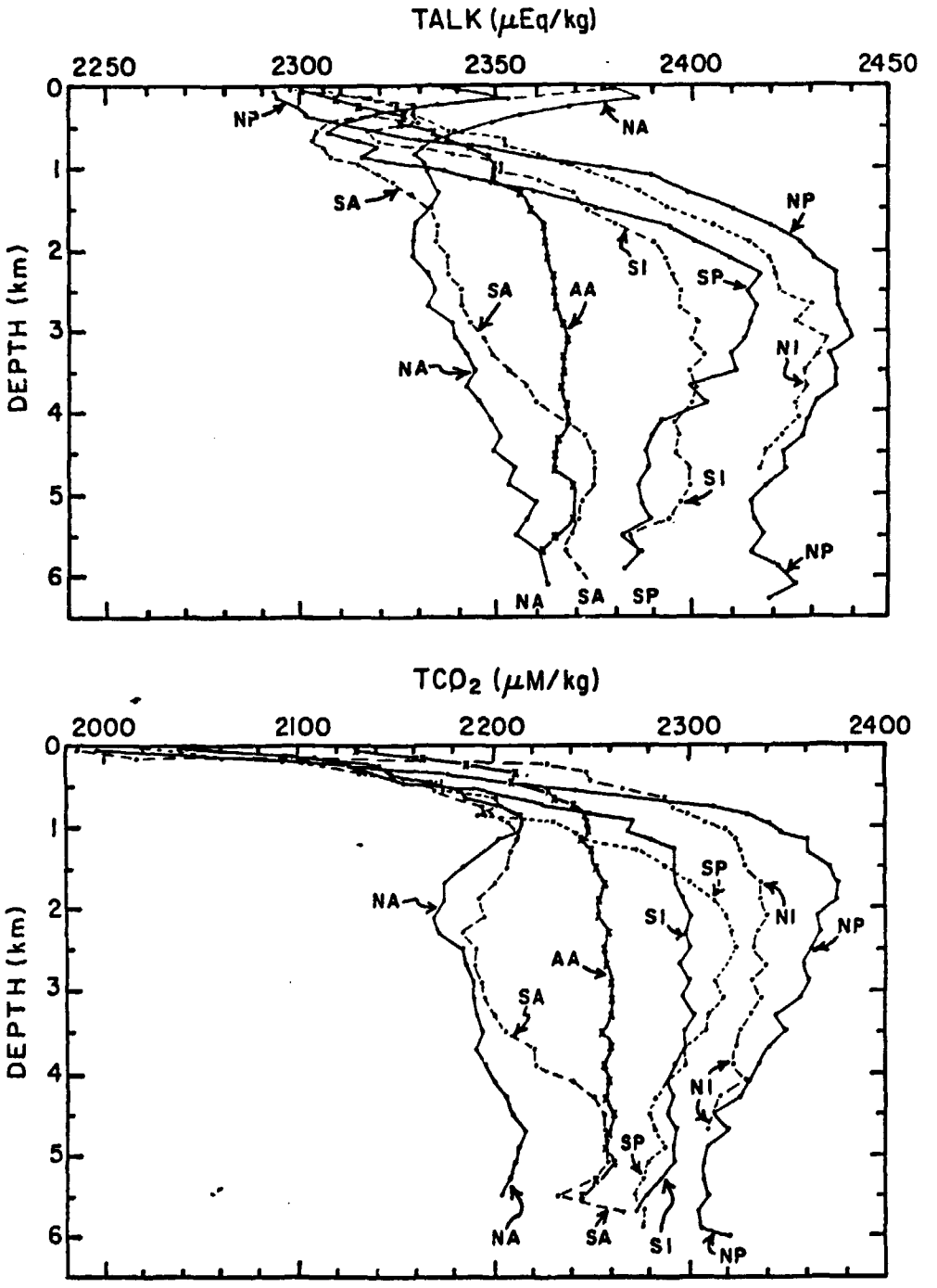

Fig. 5.1: The mean vertical distribution of (a) the alkalinity ("TALK") and (b) the total DIOC concentration ("TCO_2") in the seven regions of the world oceans. NA = North Atlantic, SA = South Atlantic, NP = North Pacific, SP = South Pacific, NI = North Indian, SI = South Indian, and AA = Antarctic region (south of 45°S). The mean values for each depth intervals in the first six oceanic regions are indicated by solid circles, and those in the Antarctic region are indicated by X's. (Taken from Takahashi et al. [1981]).

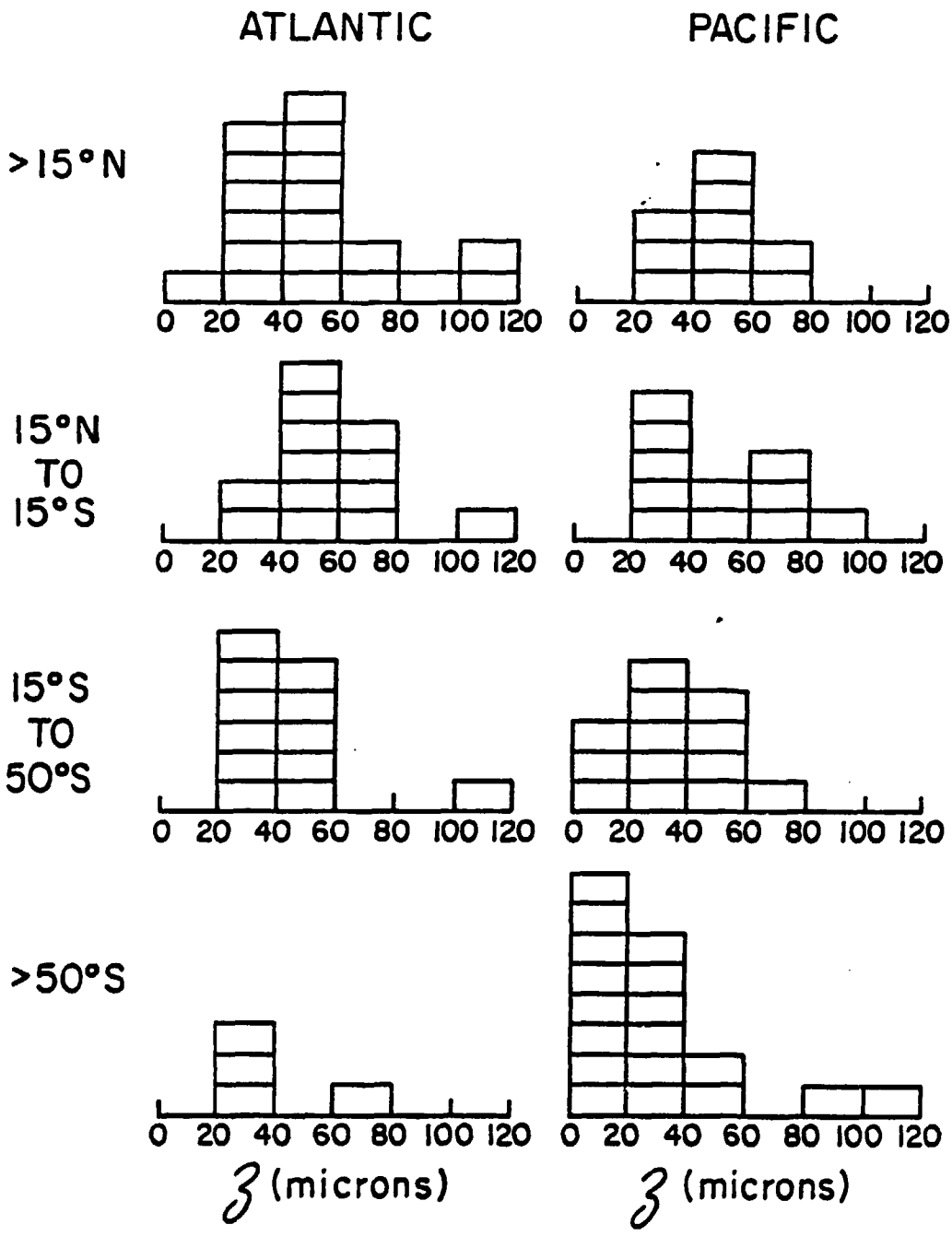

Fig. 5.2: Histograms of stagnant film-thickness estimates based on GEOSECS radon measurements in the surface waters of the Atlantic and Pacific Oceans. The measurements are separated according to latitude band. There is a suggestion that the exchange rate is somewhat lower than average in the equatorial zone (15°S to 15°N) and somewhat higher than average in the Antarctic zone (>50°S). (Taken from Broecker and Peng [1982, p. 126]).

6. SUMMARY

From the information reviewed above, the oceanic inventory for natural ^{14}C is $19,600 \times 10^{26}$ atoms (Table 4.3) and this inventory is similar to estimates predicted by other methods. The natural production rate of ^{14}C in the atmosphere is currently about 3×10^{26} atoms yr^{-1}. By 1950 the natural atmospheric ^{14}C activity had declined by about 3% as a result of the burning of fossil fuels, a decline commencing in the 19th century (Suess effect).

The oceanic inventory in 1972 of ^{14}C produced from nuclear weapons is estimated to be 303×10^{26} atoms (Table 4.3). Since the total production of ^{14}C from nuclear weapons itself is estimated to be 550×10^{26} atoms, the above figure indicates that some 52% of that activity was in the oceans in 1972. At that time, at least 181×10^{26} atoms of ^{14}C was still in the atmosphere (table 3.1) and presumably up to 65×10^{26} ^{14}C atoms would have gone into the biosphere. Between 1972 and 1985, some 132×10^{26} atoms of bomb ^{14}C have been added to the earth's oceans, as estimated in section 5.5 resulting in an inventory of 435×10^{26} atoms in 1985.

In 1985 some 82×10^{26} atoms of bomb ^{14}C remain in the atmosphere and most of this will transfer to the ocean at about 6% per year. If there are no further atmospheric nuclear tests the atmospheric excess ^{14}C will slowly decline at the above rate.

However there will be an increasing input of man-made ^{14}C discharged into the atmosphere from the nuclear power industry. Current production is about 0.5×10^{26} atoms $^{14}C/yr$ which is some 17% of the natural ^{14}C production rate. Although this source is small compared with current bomb ^{14}C inventories in the ocean and in the atmosphere it will become more significant in the future if the nuclear power industry expands significantly.

The exchange rate of radiocarbon between the atmosphere and the ocean can be determined from modelling atmospheric and oceanic levels of ^{14}C or can be estimated more directly by determining the invasion rate of CO_2 molecules between the atmosphere and surface ocean. Most of the carbon exchange models predict an exchange time of carbon from the atmosphere to the ocean of about seven years, and this agrees with other estimates which gives an average invasion rate between the atmosphere and the surface ocean of 22 moles m^{-2} yr^{-1}. The rate of change of the atmospheric bomb ^{14}C inventory in 1985 (fig. 3.1), of -6% per year, indicates that from 4 to 5×10^{26} atoms of bomb ^{14}C per year are being added to the ocean.

As can be seen from fig. 4.8, the oceanic distribution of bomb ^{14}C in surface water is far from uniform. Generally concentrations are higher in low to mid latitude regions, particularly in those areas of the ocean where there is a relatively shallow thermocline. Concentrations are lower in areas of upwelling and where there is strong convective mixing with deep ocean waters as in the oceans surrounding Antarctica. Figs 4.5 and 4.6 indicate that although bomb ^{14}C had mixed into the surface ocean and into the thermocline regions by 1970, much of the deep ocean retained ^{14}C levels similar to those prevailing prior to nuclear testing.

Over the next few centuries present variations in oceanic ^{14}C distribution will become smooth and will ultimately reflect the age structure of ocean waters. The present concentration of bomb-carbon in the atmosphere and surface oceans will decline and the global distribution of ^{14}C will show uniform increase of about 2.5% due to nuclear testing.

The GEOSECS survey of oceanic ^{14}C gave a very good snapshot of its distribution in the 1970s. There is a need for further surveys in the future to verify the time evolution of the distribution of ^{14}C in the world's oceans. A continuing international effort is also needed to monitor ^{14}C in the atmosphere in order to verify future releases from the nuclear power industry and in this respect monitoring the difference between the northern and southern hemispheres is particularly relevant.

ACKNOWLEDGEMENTS

The authors wish to acknowledge the help of Miss Shirley Stuart and Mrs Anne Hepenstall for assisting with the typing and laying out of this report.

REFERENCES

Bacastow, R.B. and Bjorkstrom, A., "Comparison of ocean models for the carbon cycle", in Carbon Cycle Modelling (SCOPE 16), edited by B. Bolin, pp29-79, John Wiley, New York, 1981.

Bacastow, R.B. and Keeling C.D., "Models to predict future atmospheric CO_2 concentrations" in proc. Workshop on the Global Effects of Carbon Dioxide from Fossil Fuels, edited by W.P. Elliot and L. Machta, pp72-90, USDoE Rep. CONF-770385, 1979.

Baes, C.F., Bjorkstrom, A. and Mulholland, P.J., "Uptake of carbon dioxide by the oceans", in Atmospheric Carbon Dioxide and the Global Carbon Cycle, edited by J.R. Trabalka, pp81-111, USDoE Rep. DOE/ER-0239, 1985.

Bien, G. and Suess, H., "Transfer and exchange of ^{14}C between the atmosphere and the surface water of the Pacific Ocean", in Radioactive Dating and Methods of Low-level Counting, pp105-115, IAEA, Vienna, 1967.

Bien, G.S., Rakestraw, N.W. and Suess, H., "Radiocarbon in the Pacific and Indian Oceans and its relation to deep water movements", Limnol. Oceanogr., 10 (Suppl.), R25-R37, 1965.

Bjorkstrom, A., "A model of CO_2 interaction between atmosphere, oceans, and land biota", in The Global Carbon Cycle (SCOPE 13), edited by B. Bolin, E.T. Degens, S. Kempe and P. Ketner, pp403-457, John Wiley, New York, 1979.

Bolin, B., "On the exchange of cabon dioxide between the atmosphere and the sea", Tellus, 12, 274-281, 1960.

Bolin, B., Bjorkstrom, A., Keeling, C.D., Bacastow, R. and Siegenthaler, U., "Carbon Cycle Modelling", in Carbon Cycle Modelling (SCOPE 16), edited by B. Bolin, pp1-28, John Wiley, New York, 1981.

Brewer P.G., Sarmiento, J.L. and Smethie, W.M., "The Transient Tracers in the Ocean (TTO) program: the North Atlantic study, 1981; the tropical Atlantic study, 1983", J. Geophys. Res., 90, 6903-6905, 1985.

Broecker, W.S. and Li, Y.-H., "Interchange of water between the major oceans", J. Geophys. Res., 75, 3545-3552, 1970.

Broecker, W.S. and Peng, T.-H., "The vertical distribution of radon in the BOMEX area", Earth Planet. Sci. Lett., 11, 99-108, 1971.

Broecker, W.S. and Peng, T.-H., "Gas exchange rates between air and sea", Tellus, 26, 21-35, 1974.

Broecker, W.S. and Peng, T.-H., "Seasonal variability in the $^{14}C/^{12}C$ ratio for surface ocean water", Geophys. Res. Lett., 7, 1020-1022, 1980.

Broecker, W.S. and Peng, T.-H., "A strategy for the development of an improved model for the uptake of fossil fuel CO_2 by the ocean", in Carbon Cycle Modelling (SCOPE 16), edited by B. Bolin, pp223-226 John Wiley, New York, 1981.

Broecker, W.S. and Peng, T.-H., "Tracers in the sea", Eldigio Press, Palisades, New York, 690pp, 1982.

Broecker, W.S., Gerard, R., Ewing, M., and Heezen, B.C., "Natural radiocarbon in the Atlantic Ocean", J. Geophys. Res., 65, 2903-2931, 1960.

Broecker, W.S. Li, Y.H. and Cromwell, J., "Radium-226 and Radon-222: concentrations in Atlantic and Pacific Oceans", Science, 158, 1307-1310, 1967.

Broecker, W.S., Peng, T.-H. and Stuiver, M., "An estimate of the upwelling rate in the equatorial Atlantic based on the distribution of bomb radiocarbon", J. Geophys. Res., 83, 6179-6186, 1978.

Broecker, W.S., Takahashi, T., Simpson, H.J. and Peng, T.-H., "Fate of fossil fuel carbon dioxide and the global carbon budget", Science, 206, 409-418, 1979.

Broecker, W.S., Peng, T.-H. and Enge, R., "Modeling the carbon system", Radiocarbon, 22, 565-598, 1980a.

Broecker, W.S., Peng, T.-H. and Takahashi, T., "A strategy for the use of bomb-produced radiocarbon as a tracer for the transport of fossil fuel CO_2 into the deep-sea source regions", Earth Planet. Sci. Lett., 49, 463-468, 1980b.

Broecker, W.S., Peng, T.-H., Mathieu, G., Hesslein, R. and Torgersen, T., "Gas exchange rate measurements in natural systems", Radiocarbon, 22, 676-683, 1980c.

Broecker, W.S., Peng, T.-H., Ostlund, G. and Stuiver, M., "The distribution of bomb radiocarbon in the ocean", J. Geophys. Res., 90, 6953-6970, 1985.

Craig, H., "The natural distribution of radiocarbon and the exchange time of carbon dioxide between atmosphere and sea", Tellus, 9, 1-17, 1957.

Craig, H., "Abyssal carbon and radiocarbon in the Pacific", J. Geophys. Res., 74, 5491-5506, 1969.

Craig, H. and Weiss, R.F., "The GEOSECS 1969 intercalibration station: introduction and hydrographic features, and total CO_2-O_2 relationships", J. Geophys. Res., 75, 7641-7647, 1970.

Crane, A.J., "The partitioning of excess CO2 in a five-reservoir atmosphere-ocean model", Tellus, 34, 398-401, 1982.

Damon, P.E., Lerman, J.C. and Long, A., "Temporal fluctuations of atmospheric ^{14}C: Causal factors and implications", Ann. Rev. Earth and Planet. Sci., 6, 457-494, 1978.

Deacon, E.L., "Gas transfer to and across an air-water interface", Tellus, 29, 363-374, 1977.

Delibrias, G., "Carbon-14 in the southern Indian Ocean", Radiocarbon, 22, 684-692, 1980.

Druffel, E.M., "Radiocarbon in annual coral rings of Belize and Florida", Radiocarbon, 22, 363-371, 1980

Druffel, E.M., "Radiocarbon in annual coral rings from the eastern tropical Pacific Ocean", Geophys. Res. Lett., 8, 59-62, 1981.

Druffel, E.M., "Banded corals: changes in oceanic carbon-14 during the little ice-age", Science, 218, 13-19, 1982.

Druffel, E.M. and Linick, T.W., "Radiocarbon in annual coral rings of Florida", Geophys. Res. Lett., 5, 913-916, 1978.

Druffel, E.M. and Suess, H.E., "On the radiocarbon record in banded corals: exchange parameters and net transport of $^{14}CO_2$ between atmosphere and surface ocean", J. Geophys. Res., 88, 1271-1280, 1983.

Emanuel, W.R., Fung, I.Y.-S., Killough, G.G., Moore, B. and Peng, T.-H., "Modeling the global carbon cycle and changes in the atmospheric carbon dioxide levels", in Atmospheric Carbon Dioxide and the Global Carbon Cycle, edited by J.R. Trabalka, pp141-173, USDoE Rep. DOE/ER-0239, 1985.

Enting, I.G. and Pearman, G.I., "Description of a one-dimensional global carbon cycle model", Div. Atmos. Phys., (Technical Paper No. 42), CSIRO, Canberra, Australia, 1982.

Enting, I.G. and Pearman, G.I., "Refinements to a one-dimensional carbon cycle model", Div. Atmos. Res., (Technical Paper No. 3), CSIRO, Canberra, Australia, 1983.

Fairhall, A.W., "Radiocarbon in the sea", Prog. Rep. 15/Aug/68-1/May/71, University of Washington Rep. RLO-2225-T20-3 (avail. from NTIS), 1971.

Fairhall, A.W., "Radiocarbon in the sea", Prog. Rep. 15/Aug/68-1/May/74, University of Washington Rep. RLO-2225-T20-10 (avail. from NTIS), 1974.

Fairhall, A.W., "Radiocarbon in the sea", Final Rep., University of Washington Rep. RLO-2225-T20-12 (avail. from NTIS), 1975.

Fairhall, A.W. and Young, A.W., "Historical ^{14}C measurements for the Atlantic, Pacific and Indian Oceans", Radiocarbon, 27, 473-507, 1985.

Fairhall, A.W., Young, A.W. and Bradford, P.A., "Radiocarbon in the sea", in proc. 8th Int. Conf. on Radiocarbon Dating, Wellington N.Z., pp C2-C42, Royal Soc. of N.Z., 1972.

Fiadeiro, M., "The alkalinity of the deep Pacific", Earth Planet. Sci. Lett. 49, 499-505, 1980.

Glasstone, S. and Dolan, P.J., "The effects of nuclear weapons", Castle House Publications, Tunbridge Wells, England, 653pp, 1977.

Gordon, A.L., "Interocean exchange of thermocline water", J. Geophys. Res., 91, 5037-5046, 1986.

Grey, D., "Fluctuations of atmospheric radiocarbon", Ph.D. Thesis, Univ. of Ariz., Tucson. (Also available from Univ. Microfilms, Ann Arbor, Mich), 1972.

Hoffert, M.I., Callegari, A.J. and Hsieu, C.-T., "A box-diffusion carbon cycle model with upwelling, polar bottom water formation and a marine biosphere", in Carbon Cycle Modelling (SCOPE 16), edited by B. Bolin, pp287-305, John Wiley, New York, 1981.

Holmen, K. and Liss, P., "Models for air-water gas transfer: an experimental investigation", Tellus, 36B, 92-100. 1984.

Kanwisher, J., "On the exchange of gases between the atmosphere and the sea", Deep-Sea Res., 10, 195-207, 1963.

Killough, G.G. and Emanuel, W.R., "A comparison of several models of carbon turnover in the ocean with respect to their distributions of transit time and age, and responses to atmospheric CO_2 and ^{14}C", Tellus, 33, 274-290, 1981.

Kroopnick, P., "Correlations between ^{13}C and CO_2 in surface waters and atmospheric CO_2", Earth Planet. Sci. Lett., 22, 397-403, 1974a.

Kroopnick, P., "The dissolved O_2-CO_2-^{13}C system in the eastern equatorial Pacific", Deep-Sea Res., 21, 211-227, 1974b.

Kroopnick, P., "The distribution of ^{13}C in the Atlantic Ocean", Earth Planet. Sci. Lett., 49, 469-484, 1980.

Levin, I., Kromer, B., Schoch-Fischer, H., Bruns, M., Munnich, M., Berdau, D., Vogel, J.C. and Munnich, K.O., "25 years of tropospheric ^{14}C observations in central Europe", Radiocarbon, 27, 1-19, 1985.

Lingenfelter, R.E. and Ramaty, R., "Astrophysical and geophysical variations in ^{14}C production", in Radiocarbon Variations and Absolute Chronology (Nobel Symp. 12), edited by I.U. Olsson, pp513-537, John Wiley, New York, 1970.

Linick, T.W., "La Jolla measurements of radiocarbon in the oceans", Radiocarbon, 20, 333-359, 1978.

Linick, T.W., "Bomb-produced carbon-14 in the surface water of the Pacific Ocean", Radiocarbon, 22, 599-606, 1980.

Machta, L., List, R.J., and Telegadas, K., "Meteorology of fallout from 1961-1962 nuclear test", Congress of the United States, Hearing

before subcommittee in Research, Development and Radiation of the joint committee of Atomic Energy, 88th Congress 46-61, June 1963.

Manning, M.R., Jansen, H.S., McGill, R.C., and Burr, M.K., "A summary of atmospheric carbon 14 measurements made in the South Pacific from 1954 to 1985", Institute of Nuclear Sciences, DSIR, New Zealand, (in preparation) 1986.

Munnich, K.O. and Roether, W., "Transfer of bomb ^{14}C and tritium from the atmosphere to the ocean. Internal mixing of the ocean on the basis of tritium and ^{14}C profiles", in Radioactive Dating and Methods of Low-level Counting, pp93-104, IAEA, Vienna, 1967.

Nozaki, Y., Rye, D.M., Turekian, K.K. and Dodge, R.E., "A 200 year record of carbon-13 and carbon-14 variations in a Bermuda coral", Geophys. Res. Lett., 5, 825-828, 1978.

Nydal, R., Gulliksen, S., Lovseth, K. and Skogseth, F.H., "Bomb ^{14}C in the ocean surface 1966-1981", Radiocarbon, 26, 7-45, 1984.

O'Brien, K., "Secular variations in the production of cosmogenic isotopes in the earth's atmosphere", J. Geophys. Res. 84, 422-431, 1979.

Oeschger, H., Siegenthaler, U., Schotterer, U. and Gugelmann, A., "A box diffusion model to study the carbon dioxide exchange in nature", Tellus, 27, 168-192, 1975.

Ostlund, H.G. and Stuiver, M., "GEOSECS Pacific Radiocarbon", Radiocarbon, 22, 25-53, 1980.

Peng, T.-H., "Uptake of anthropogenic CO_2 by lateral transport models of the ocean based on the distribution of bomb-produced ^{14}C", Radiocarbon, 28, 363-375, 1986.

Peng, T.-H., Takahashi, T. and Broecker, W.S., "Surface radon measurements in the North Pacific Ocean station PAPA", J. Geophys. Res., 79, 1772-1780, 1974.

Peng, T.-H., Broecker, W.S., Mathieu, G.G. and Li, Y.-H., "Radon evasion rates in the Atlantic and Pacific Oceans as determined during the GEOSECS program", J. Geophys. Res., 84, 2471-2486, 1979.

Quay, P. D. and Stuiver, M., "Vertical advection-diffusion rates in the oceanic thermocline determined from ^{14}C distributions", Radiocarbon, 22, 607-625, 1980.

Quay, P. D., Stuiver, M. and Broecker, W.S., "Upwelling rates for the equatorial Pacific Ocean derived from the bomb ^{14}C distribution", J. Mar. Res., 41, 769-792, 1983.

Quinn, J.A. and Otto, N.C., "Carbon dioxide exchange at the air-sea interface: flux augmentation by chemical reaction", J. Geophys. Res., 76, 1539-1549, 1971.

Rafter, T.A. and O'Brien, B.J., "Exchange rates between the atmosphere and the ocean as shown by recent ^{14}C measurements in the South Pacific", in Radiocarbon Variations and Absolute Chronology (Nobel Symp. 12), edited by I.U. Olsson, pp355-377, John Wiley, New York, 1970.

Siegenthaler, U., "Uptake of excess CO_2 by an outcrop-diffusion model of the ocean", J. Geophys. Res., 88, 3599-3608, 1983.

Siegenthaler, U. and Oeschger, H., "Predicting future atmospheric carbon dioxide levels", Science, 199, 388-395, 1978.

Smethie, W.M., Takahashi, T. and Chipman, D.W., "Gas exchange and CO_2 flux in the tropical Atlantic Ocean determined from ^{222}Rn and pCO_2 measurements", J. Geophys. Res., 90, 7005-7022, 1985.

Stuiver, M., "The ^{14}C cycle and its implications for mixing rates in the ocean-atmosphere system", in Carbon and the Biosphere, edited by G.M. Woodwell and E.V. Pecan, pp6-20, USAEC Rep. CONF-720510.

Stuiver, M., "^{14}C distribution in the Atlantic Ocean", J. Geophys. Res., 85, 2711-2718, 1980a.

Stuiver, M., "Workshop on ^{14}C reporting", Radiocarbon, 22, 964-966, 1980b.

Stuiver, M. and Ostlund, H.G., "GEOSECS Atlantic Radiocarbon", Radiocarbon, 22, 1-24, 1980.

Stuiver, M. and Ostlund, H.G., "GEOSECS Indian Ocean and Mediterranean Radiocarbon", Radiocarbon, 25, 1-29, 1983.

Stuiver, M. and Polach, H.A., "Reporting of ^{14}C data", Radiocarbon, 19, 355-363, 1977.

Stuiver, M. and Quay, P.D., "Atmospheric ^{14}C changes resulting from fossil fuel CO_2 release and cosmic ray flux variability", Earth Planet. Sci. Lett. 53, 349-362, 1981.

Stuiver, M., Ostlund, H.G. and McConnaughey, T.A., "GEOSECS Atlantic and Pacific ^{14}C distribution", in Carbon Cycle Modelling (SCOPE 16), edited by B. Bolin, pp201-221, John Wiley, New York, 1981.

Stuiver, M., Quay, P.D. and Ostlund, H.G., "Abyssal water carbon-14 distribution and the age of the world oceans", Science, 219, 849-851, 1983.

Suess, E., "Particulate organic carbon flux in the oceans - surface productivity and oxygen utilization", Nature, 288, 260-263, 1980.

Suess, H.E., "Secular variations of the cosmic-ray produced carbon 14 in the atmosphere and their interpretations", J. Geophys. Res. 70, 5937-5952, 1965.

Takahashi, T. and Azevedo, A.E.G., "The oceans as a CO_2 reservoir", in Interpretation of Climate and Photochemical Models, Ozone and

Temperature, edited by R.A. Peck and J.R. Hummel, pp83-109, Amer. Inst. Physics conf. proc. no. 82, 1982.

Takahashi, T., Kaiteris, P., Broecker, W.S. and Bainbridge, A.E., "An evaluation of the apparant dissociation constants of carbonic acid in sea water", Earth Planet. Sci Lett., 32, 458-467, 1976.

Takahashi, T., Broecker, W.S. and Bainbridge, A.E., "The alkalinity and total carbon dioxide concentration in the world oceans", in Carbon Cycle Modelling (SCOPE 16), edited by B. Bolin, pp271-286, John Wiley, New York, 1981.

Telegadas, K., "The seasonal atmospheric distribution of excess carbon 14 from March 1955 to July 1969", in Health and Safety Lab. Rep. HASL-243, USAEC, 1971.

UNSCEAR, "Sources and Effects of Ionizing radiation, report of the United Nations Scientific Committee on the Effects of Atomic Radiation, p119, United Nations, New York, 1977.

UNSCEAR, "Ionizing Radiation Sources and Biological Effects", report of the United Nations Scientific Committee on the Effects of Atomic Radiation, p259, United Nations, New York, 1982.

Wannikhof, R., Ledwell, J. and Broecker, W.S., "Gas exchange - wind speed relation measured with sulfur hexafluoride on a lake", Science, 1224-1226, 1985.

Wunsch, C., "An estimate of the upwelling rate in the equatorial Atlantic based on the distribution of bomb radiocarbon and quasi-geostrophic dynamics", J. Geophys. Res., 89, 7971-7978, 1984.